Plant Stress 18 (2025) 101013

Contents lists available at ScienceDirect

Plant Stress

journal homepage: www.sciencedirect.com/journal/plant-stress

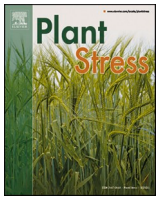

Heat tolerance in *Arabidopsis thaliana* seedlings requires functional DMS3, a component of *de novo* methylation

Sandra Vitko [a], Mirta Tokić [a], Silvia Braun [b], Thorsten Brehm [b], Iva Pavlović [c], Fabio Fiorani [b], Ondřej Novák [c], Nataša Bauer [a], Dunja Leljak-Levanić [a], Željka Vidaković-Cifrek [a,*]

[a] Department of Biology, Faculty of Science, University of Zagreb, Horvatovac 102a, 10000 Zagreb, Croatia
[b] Institute of Bio- and Geosciences (IBG), Plant Sciences (IBG-2), Forschungszentrum Jülich GmbH, Wilhelm-Johnen-Straße, 52428 Jülich, Germany
[c] Laboratory of Growth Regulators, Faculty of Science, Palacký University and Institute of Experimental Botany, Czech Academy of Sciences, Šlechtitelů 27, 77900 Olomouc, Czech Republic

ARTICLE INFO

Keywords:
RdDM
DMS3
Thermotolerance
JIP-test
High-throughput phenotyping
Hormonal profile

ABSTRACT

The protein Defective in RNA-directed DNA Methylation 3 (DMS3) is part of RNA-directed DNA methylation, an epigenetic mechanism involved in the regulation of plant development and stress response. However, the specific role of the DMS3 protein in thermotolerance remains unclear. To determine how altered *DMS3* expression and functionality affects thermotolerance, *DMS3*-overexpressor (*oeDMS3*), *DMS3*-mutant (*dms3-1*) and wild-type *Arabidopsis thaliana* seedlings were heat-treated and analyzed, focusing on morphological, physiological, biochemical and molecular changes. The *dms3-1* line showed the highest thermosensitivity after short-term exposure to 45 °C for 45 min. However, both *dms3-1* and *oeDMS3* showed a greater reduction in morphological traits compared to wild type after exposure to 40 °C for 6 h. Hormonal profiling showed that the *dms3-1* and *oeDMS3* lines had similar hormonal profiles characterized by lower jasmonate levels compared to wild type, both under stress and control conditions. The heat-stressed *dms3-1* line contained increased cytokinin levels predominantly in the form of ribosides, and also accumulated inactive auxin metabolites. Exposure to 37 °C for 24 h destabilized and altered the localization of the DMS3 protein in the root tissue. After exposure to 37 °C for 6 h, the *dms3-1* line showed a delayed recovery of reduced photosynthetic efficiency, accompanied by a partial activation of the antioxidant system and increased proline content. Under control conditions, *dms3-1* plants exhibited reduced growth and lower expression of RuBisCO, HSP90 and HSP70 proteins. Overall, our results suggest a crucial role of DMS3 in thermotolerance, hormone balance, antioxidant defense and photosynthetic efficiency, indicating the importance of a functional and balanced DMS3 protein for thermotolerance and for plant growth and development under control conditions.

1. Introduction

Protein Defective in RNA-directed DNA methylation 3 (DMS3) belongs to the Structural maintenance of chromosomes (SMC) hinge-domain-containing protein family, which are known for regulating genome dynamics and stability through the organization and modification of chromatin (Kanno et al., 2008; Matityahu and Onn, 2018). As part of the RNA-directed DNA methylation (RdDM) mechanism, DMS3 forms the DRD1-DMS3-RDM1 (DDR) complex with the proteins Defective in RNA-directed DNA methylation 1 (DRD1) and RNA-directed DNA methylation 1 (RDM1). DDR complex is essential for the recruitment of Domains rearranged methyltransferase 2 (DRM2), a DNA methyltransferase responsible for initiating *de novo* methylation of cytosines in all sequence contexts (CG, CHG, and CHH, where H represents A, C, or T) (Erdmann and Picard, 2020; Matzke et al., 2015; Wongpalee et al., 2019). RdDM is particularly important for silencing transposable elements and other repetitive sequences, that can relocate within the genome via various mechanisms, potentially disrupting protein-coding or regulatory sequences (Dubin et al., 2018; Erdmann and Picard, 2020; Vuković et al., 2025). For instance, Ito et al. (2011) demonstrated increased expression of the RdDM-targeted *ONSEN* retrotransposon in *Arabidopsis thaliana* plants with impaired biosynthesis of small RNAs, which is the first step of the RdDM mechanism. Furthermore, RdDM is increasingly recognized as a regulator of the expression of

* Corresponding author.
E-mail address: zeljka.vidakovic-cifrek@biol.pmf.unizg.hr (Ž. Vidaković-Cifrek).

https://doi.org/10.1016/j.stress.2025.101013

Available online 27 August 2025

stress-responsive genes, ensuring that plants can adapt to and survive adverse conditions (Palomar et al., 2021; Rowley et al., 2017; Rymen et al., 2020). Indeed, Popova et al. (2013) linked impaired RdDM to reduced basal thermotolerance in *A. thaliana*.

Heat stress disrupts metabolic balance in plants and leads to changes at the morphological, physiological, and cellular levels, including reduced leaf area, inhibited growth, impaired photosynthesis, disruption of membrane structure and fluidity, and denaturation and aggregation of cellular proteins (Fahad et al., 2017; Wani and Kumar, 2020; Zhao et al., 2021). Photosynthesis is very sensitive to elevated temperature, and often inhibited before other processes are affected. Structure and function of photosystem II (PSII) and the activity of enzyme ribulose-1,5-bisphosphate carboxylase/oxygenase (RuBisCO) are particularly sensitive to high temperatures (Mathur et al., 2014). Unfavorable temperatures also increase synthesis of reactive oxygen species (ROS), which can affect plants in two ways (Ohama et al., 2017; Wani and Kumar, 2020). As signaling molecules, ROS activate heat shock factors (HSF), which regulate the expression of various genes involved in promoting plant resistance to elevated temperatures (Mittler et al., 2012). However, due to their high reactivity, ROS can also damage essential biological molecules such as nucleic acids, proteins, and lipids (Møller et al., 2007). To restore redox balance and quench excess ROS, the activity of the antioxidant system, which includes various enzymatic and non-enzymatic molecules, is stimulated in the cells (Mittler, 2002). In recent years, several studies (Elewa et al., 2017; Qirat et al., 2018; Sadeghipour, 2020) have highlighted the amino acid proline as part of the plant antioxidant system. In addition to activating the antioxidant network, plants undergo several changes in their transcriptome, proteome and metabolome to adapt to elevated temperatures (Mittler and Blumwald, 2015; Raza et al., 2023). An important response is the induction of heat shock proteins (HSPs), which act as molecular chaperones and prevent protein aggregation or denaturation, facilitate ATP-dependent protein folding, play a role in signal transduction and gene activation, osmolyte production and regulation of the cellular redox state (Andrási et al., 2021; Kotak et al., 2007; Mittler, 2002). Phytohormones also play key roles in heat stress acclimatization (Peleg and Blumwald, 2011). Abscisic acid (ABA), for example, is known for its role in signaling pathways that regulate the expression of stress-related genes, increase the production of ROS and promote senescence, while cytokinins delay the onset of senescence and positively influence heat stress tolerance in *A. thaliana* (Grgić et al., 2025; Li et al., 2021; Prerostova et al., 2020). Furthermore, indole-3-acetic acid (IAA), the most abundant auxin in plants, has been shown to be essential for thermotolerance and thermomorphogenesis by protecting photosynthesis and reducing DNA damage (Siddiqui et al., 2017; Tognetti et al., 2012).

Although the role of the RdDM mechanism in stress responses is well-documented, the specific contribution of DMS3, particularly in the context of heat stress, remains unclear. To address this gap, our study aimed to: (1) evaluate thermosensitivity of *A. thaliana* seedlings with altered *DMS3* expression under short-term heat shock; (2) investigate plant responses to moderate, ecologically relevant heat stress; (3) assess the impact of DMS3 on plant growth and development under control conditions, as RdDM is known to regulate these processes (Erdmann and Picard, 2020; Kumar and Mohapatra, 2021). To achieve these goals, we conducted experiments in which we analyzed morphological, physiological, biochemical and molecular changes using the following approaches: (1) soil-based phenotyping to observe morphological changes from seedling to flowering stage, guiding further physiological and molecular analyses; (2) hormonal profiling on plants sampled seven days after treatment to assess long-term physiological responses; (3) *in vitro* experiments to analyze DMS3 protein stability, chlorophyll *a* fluorescence, oxidative stress markers, and seedling thermosensitivity.

2. Materials and methods

2.1. Plant material and transformation

To study the role of the DMS3 protein in heat stress response, the model plant *Arabidopsis thaliana* (L.) Heynh., ecotype Columbia, was used. Two independent lines overexpressing *DMS3* gene (*oeDMS3* 6TV6 and 4TV7) were generated as described in Jagić et al. (2022). The *GFP-DMS3* transgene was constructed under the control of the CaMV 35S promoter, which enabled the constitutive expression of the protein product of the *GFP-DMS3* transgene. In addition to the overexpressing lines, we also used a mutant line (*dms3-1*) that has a point mutation and a substitution of glycine (G) to glutamic acid (E), which is essential for the formation of an active DMS3 dimer (Kanno et al., 2008). Wild-type plants were used as control plants in comparison with *A. thaliana* plants that had altered *DMS3* gene expression. Unless otherwise stated in the Results section, the *oeDMS3* 6TV6 line was used to compare the heat stress response of *oeDMS3, dms3-1*, and wild-type plants.

2.2. Thermosensitivity test

To determine the ability of seedlings with altered *DMS3* gene expression to recover from heat shock, seedlings were grown under long-day conditions (16 h light, 8 h dark) at a temperature of 24 ± 1 °C and a light intensity of 120–130 μmol m^{-2} s^{-1} on solid MS medium according to Murashige and Skoog (1962) and with the addition of 2 % (w/v) sucrose and 1 % (w/v) agar. Seven-day-old seedlings were exposed to a temperature of 45 °C for 45 min. The intensity and duration of the heat shock was determined in a preliminary experiment in which the *A. thaliana* seedlings were exposed to 45 °C for 30 min, 45 min or 75 min in order to find suitable conditions that did not cause immediate lethality. The ability of the seedlings to recover was evaluated for seven days after treatment. Seedlings were considered viable if they continued to develop true leaves and elongate the epicotyl. The survival percentage of seedlings was calculated as the ratio of surviving seedlings to the total number of seedlings and multiplied by 100. Control seedlings of each line were grown at 24 °C throughout the experiment and their survival percentage was considered 100 %.

2.3. High-throughput phenotyping

To investigate the effects of heat stress and altered *DMS3* gene expression on growth and development of *A. thaliana* plants from seedling stage to flowering stage, morphological traits (Suppl. Fig. 1) and chlorophyll fluorescence were monitored using the GROWSCREEN chamber phenotyping system (Barboza-Barquero et al., 2015; Jansen et al., 2009; Prerostova et al., 2018). About 250 seeds of each line were sown in pots with soil substrate (Fruhstorfer Erde, Hawita). To promote and synchronize germination, the pots with seeds were stratified at a temperature of 4°C for three days. After stratification, the pots were transferred to the GROWSCREEN chamber under long-day conditions at a temperature of 24 ± 1 °C, a light intensity of 180–220 μmol m^{-2} s^{-1}, a CO_2 concentration of 400 ppm, and air humidity of 60 %. On the fifth day of growth, using an automated seedling detection system inside the GROWSCREEN chamber (Scharr et al., 2020), 40 uniform seedlings from each line were selected and transplanted into individual pots with soil substrate. Five days later, the seedlings were divided into two groups. The first group was the control group (C), which grew at a temperature of 24 °C throughout the experiment, while the second group (HS) was exposed to a temperature of 40 °C for 6 h at the developmental stage with two true leaves (developmental stage 1.02; defined according to Boyes et al., 2001). After treatment, seedlings were returned to 24 °C. An automated system inside the GROWSCREEN chamber weighed plant pots daily to monitor soil substrate moisture. Based on these data, plants were watered with tap water as needed to maintain soil moisture between 40 % and 70 % of substrate water holding capacity. This watering

regime prevented water shortage for both control and heat-treated plants. The plants were observed daily from the day before treatment until flowering. Morphological parameters were recorded daily, except on the day of treatment and weekends, while PAM fluorescence parameters were measured twice: immediately after heat treatment and again two days later in dark-adapted plants. Seven days after treatment, plants were sampled for hormonal analysis. At the end of the experiment, the remaining plants were collected, dried at 70 °C for three days, and their dry weight was measured.

2.4. Hormonal profile screening

Hormonal analysis was performed on plants grown in soil as described in Section 2.3. Plants were treated at the two-leaf stage and sampled for the analysis seven days after heat treatment. A protocol developed by Šimura et al. (2018) was used for the quantification of plant hormones and their metabolites. In brief, 2 mg of dried plant material per sample was combined with stable isotope-labeled internal standards and extracted in 1 mL of cold 50 % (v/v) acetonitrile (ACN) using a mixer mill (27 Hz for 5 min, MM 301, Retsch, Germany), followed by sonication (3 min at 4 °C, Transsonic T310, Elma) and extraction in a laboratory rotator (30 min at 4 °C, Stuart SB3, Bibby Scientific). After centrifugation (10 min, 36,670 × g and 4 °C), the supernatant was purified using Oasis HLB solid-phase extraction cartridges (1 cc per 30 mg, Waters) prewashed with 1 mL of 100 % methanol and 1 mL of deionized water and then equilibrated with 50 % ACN. The samples were then loaded into the cartridges, and the flow-through fraction was collected along with a 30 % ACN rinse, combined and evaporated to dryness under nitrogen (TurboVap LV evaporator, Caliper Life Sciences). Prior to analysis, the samples were dissolved in 40 μL of 30 % ACN and filled into vials fitted with micro-inserts. The target compounds were analyzed using an Acquity UPLC I-Class system (Waters) coupled to a Xevo TQ-S triple quadrupole mass spectrometer (Waters). The mobile phase for UPLC consisted of binary gradients of ACN with 0.01 % (v/v) formic acid and 0.01 % (v/v) aqueous formic acid, with a flow rate of 0.5 mL min^{-1}. MassLynx software (version 4.1, Waters) was used for acquisition and processing of mass spectrometry data.

2.5. DMS3 protein stability and localization

To assess the stability and localization of the DMS3 protein, *A. thaliana* seedlings overexpressing *DMS3* gene were grown as described in Section 2.2. After five days, seedlings were subjected to a temperature treatment at 37 °C for 24 h and subsequently analyzed with a confocal microscope. The control group of each line was grown at a temperature of 24 °C throughout the experiment and was analyzed at the same time point as the treated group. The roots were selected for analysis due to their lower autofluorescence and simpler structure, which facilitated imaging. Analysis was performed using Fiji ImageJ v1.54f, Java 1.8.0_322 (Schindelin et al., 2012) and followed the methodology of Gu et al. (2014). Briefly, the regions of interest (Suppl. Fig. 2) were defined by the outlines of parts of the root tip or differentiation zone characterized by the first appearance of root hairs. A single straight line (length 200 ± 0.1 pixel) was used as a reference for consistent area selection in all images. Total fluorescence was calculated using the following formula: Integrated density of selected region – (Area of selected region × Mean fluorescence of background), giving results in arbitrary units (a.u.). These were expressed as relative GFP intensities (RGI) normalized to control samples, which were set as one.

2.6. Physiological, biochemical and molecular profiling

To gain insight into specific responses to heat stress, which included physiological, biochemical and molecular characterization, seedlings were grown on liquid MS medium.

Approximately 3.5 mg of seeds were weighed into 2 mL microtubes. A total of 20 microtubes were prepared for each line. After weighing, the seeds were sterilized, transferred to sterile Petri dishes with liquid MS medium and stratified according to the methodology described in Vuković et al. (2025). After stratification, Petri dishes with seeds were placed in the growth chamber. During the next 12 days, 1 mL of MS medium was added twice to each Petri dish under sterile conditions. On the twelfth day of growth, when the seedlings reached developmental stage 1.02 (Boyes et al., 2001), Petri dishes were divided into two groups – control and treated group. The control group remained in the growth chamber at 24 °C, while the treated group was placed in an incubator (Hood TH 30, Edmund Bühler, Germany) preheated to 37 °C. After 6 h at 37 °C, half of the Petri dishes with control (C-HS) and treated (HS) seedlings were used immediately for further physiological, biochemical, and molecular analyses, while the other half (C-REC, REC) were returned to the growth chamber and taken for analyses after a 24-h recovery period at 24 °C. Before sampling, seedlings were rinsed in distilled water to remove liquid MS medium.

2.6.1. Photosynthetic performance using JIP-test

To determine the effect of heat stress on the primary photochemistry of seedlings, chlorophyll *a* (Chl *a*) fluorescence was measured in control and heat-treated seedlings after a 30-min dark adaptation period at 24 °C using a FluorPen FP 100 fluorometer (Photon Systems Instruments, Brno, Czech Republic). To trigger the polyphasic increase in Chl *a* fluorescence, a pulse of saturated blue light (3000 μmol m^{-2} s^{-1}, peak at 455 nm) was applied. Fluorescence was recorded at 50 μs (initial value, F_0), 2 ms (F_J), 30 ms (F_I), and at peak fluorescence (F_M). OJIP transients were analyzed using the JIP-test methodology (Strasser et al., 2000), yielding various parameters describing the photochemistry of PSII. These parameters included the maximum quantum yield of PSII (F_V/F_M), absorption-based performance index (PI_{ABS}), specific energy fluxes – absorption (ABS/RC), trapping (TR_0/RC), electron transport (ET_0/RC), and dissipation of energy as heat (DI_0/RC) per active PSII reaction center (RC). Additionally, the density of active reaction centers (RC/CS_0) per excited leaf cross-section (CS_0) was determined. All parameter values were expressed in arbitrary units (a.u.).

2.6.2. Immunodetection of RuBisCO, HSP90, HSP70 and DMS3

To determine RuBisCO, HSP90 and HSP70 protein levels in control and heat-treated seedlings, ~100 mg of fresh seedlings was ground in 1 mL of ice-cold 0.1 M Tris–HCl buffer, pH 8.0 (Staples and Stahmann, 1964), supplemented with 0.5 M sucrose, 6.5 mM dithiothreitol, and 8.25 mM cysteine. During homogenization, ~10 mg of polyvinylpolypirrolidone (PVPP) was added to each sample. The homogenate was centrifuged at 20,000 × g for 30 min at 4 °C. To analyze the level of DMS3 protein in control seedlings, 150–200 mg of frozen, homogenized tissue was extracted using 400–800 μL of PEB50 extraction buffer (Škiljaica et al., 2020). Protein extracts were incubated on ice for 20–30 min with occasional mixing, followed by centrifugation at 16,000 × g for 15 min at 4 °C. The soluble protein content of both types of extracts was determined using the Bradford assay (Bradford, 1976), followed by protein denaturation in Laemmli sample buffer (Laemmli, 1970) at 95 °C for 5 min. Proteins were separated by sodium dodecyl sulfate polyacrylamide gel electrophoresis (SDS-PAGE) with a 4 % (v/v) stacking gel and a 12 % (v/v) resolving gel (T = 30 %, C = 2.66 %) using the Laemmli buffer system (Laemmli, 1970). To detect RuBisCO, *i.e.* its large subunit rbcL, HSP90 and HSP70, the proteins were electroblotted onto nitrocellulose membranes with ice-cold transfer buffer (28 mM Tris, 192 mM glycine, and 10 % (v/v) methanol, pH 8.3) at 60 V for 60 min. Membranes were then blocked for 1 h at room temperature in Tris-buffered saline (TBS-T, pH 7.5) containing 20 mM Tris, 150 mM NaCl, 1 % (v/v) Tween 20, and 5 % (w/v) non-fat dry milk. For DMS3 protein detection, proteins were transferred to polyvinylidene difluoride (PVDF) membranes overnight at 12 V and blocked for 2–3 h in 2 % (w/v) non-fat dry milk dissolved in phosphate-buffered saline (PBS, pH 7.4)

containing 137 mM NaCl, 2.7 mM KCl, 10 mM Na_2HPO_4, and 1.8 mM KH_2PO_4. After blocking, the membranes were incubated overnight at 4 °C. For the detection of RuBisCO, HSP90 and HSP70, membranes were incubated with primary rabbit anti-rbcL (Agrisera, AS03 037), anti-HSP90 (Agrisera, AS08 346) and anti-HSP70 (Agrisera, AS08 371) antibodies, diluted 1:4000, 1:3000 and 1:3000, respectively, in blocking solution. To quantify DMS3 protein levels relative to the 20S proteasome beta subunit A1 (PBA1) loading control, the membrane was cut into two parts. One part was incubated with primary rabbit anti-DMS3 (Zhong et al., 2019) diluted 1:500 in blocking solution, while the other half was incubated with primary rabbit anti-PBA1 (Enzo Biochem) diluted 1:3000. All membranes were incubated for 1–1.5 h with goat anti-rabbit HRP-conjugated secondary antibody (Sigma or EMD Millipore), diluted 1:10,000 in blocking solutions. After each antibody incubation, the membranes were washed two or three times with TBS-T and PBS buffer for 5–15 min, followed by a 5-min incubation with Immobilon Forte Western HRP chemiluminescent substrate (Merck). RuBisCO, HSP90 and HSP70 protein bands were visualized using C-DiGit Blot Scanner (LI-COR, USA) and quantified using Image Studio™ Lite 5.2 (LI-COR Biosciences – GmbH, SAD). Membranes were stained with 0.05 % (w/v) Ponceau S in 5 % (v/v) acetic acid immediately after protein transfer to serve as a loading control for RuBisCO, HSP90 and HSP70, followed by scanning (Romero-Calvo et al., 2010). DMS3 protein was visualized using autoradiographic film (Pan-G, Henry Schein®) and images were analyzed using ImageJ v.1.49 (Schneider et al., 2012) as described by Taylor and Posch (2014).

2.6.3. Oxidative stress markers

To assess the level of oxidative stress in heat-treated seedlings, the activity of four antioxidant enzymes and proline content were measured. To measure antioxidant enzyme activity, total soluble proteins were extracted by homogenizing ~150 mg of fresh seedlings with the addition of ~15 mg of PVPP in a buffer consisting of 0.1 mM ethylenediaminetetraacetic acid (EDTA) in 100 mM potassium phosphate buffer, pH 7.0. Protein concentration was determined using the Bradford assay (Bradford, 1976). Guaiacol peroxidase (G-POD, EC 1.11.1.7) activity was measured according to the method described by Maehly and Chance (1954). Briefly, the reaction mixture consisted of 980 µL of 50 mM potassium phosphate buffer (pH 7.0), 18 mM guaiacol, and 4.5 mM H_2O_2. Then, 20 µL of protein extract was added to the reaction mixture, briefly mixed, and the change in absorbance at 470 nm was measured spectrophotometrically every 15 s for 3 min. The results were calculated using the molar absorption coefficient (26.6 mM cm^{-1}) and expressed as µmol of tetraguaiacol formed per minute per milligram of total soluble protein (µmol min^{-1} mg^{-1} proteins). The activity of ascorbate peroxidase (APX, EC 1.11.1.11) was determined spectrophotometrically according to the method described by Nakano and Asada (1981). The reaction mixture consisted of 795 µL of 0.1 mM EDTA in 50 mM potassium phosphate buffer (pH 7.0), 5 µL of 20 mM ascorbate, 180 µL of protein extract, and 20 µL of 12 mM H_2O_2. The solution was mixed briefly, and the change in absorbance at 290 nm was measured every second for 15 s. The results were calculated using the molar absorption coefficient (2.8 mM cm^{-1}) and expressed as µmol of ascorbate consumed per minute per milligram of total soluble protein (µmol min^{-1} mg^{-1} proteins). Catalase (CAT, EC 1.11.1.6) activity was measured according to the method described by Aebi (1984). In short, 50 µL of protein extract was added to 950 µL of reaction mixture consisting of 50 mM potassium phosphate buffer (pH 7.0) and 10 mM H_2O_2, mixed briefly, and the change in absorbance at 240 nm was measured every 10 s for 2 min. The results were calculated using the molar absorption coefficient (40 mM cm^{-1}) and expressed as nmol H_2O_2 consumed per minute per milligram of total soluble protein (nmol min^{-1} mg^{-1} proteins). The activity of superoxide dismutase (SOD, EC 1.15.1.1) was determined spectrophotometrically using the method described by Beauchamp and Fridovich (1971). The reaction mixture consisted of 825 µL of SOD reaction buffer (5 µM NBT and 0.1 mM EDTA in 50 mM potassium phosphate buffer, pH 7.8), 75 µL of 10.8 mM xanthine, 45 µL of protein extraction buffer, 50 µL of 0.05 U mL^{-1} xanthine oxidase, and 5 µL of protein extract. The change in absorbance was measured at 560 nm every 30 s for 3 min. SOD activity was calculated using a calibration curve prepared from a range of known SOD activities (0.005–1 U $µL^{-1}$). Results were expressed as U per mg protein (U mg^{-1} protein), where U is defined as the amount of SOD required to inhibit the rate of NBT reduction by 50 %. For proline determination, ~200 mg of fresh seedlings was homogenized in 0.1 % (w/v) trichloroacetic acid. The further protocol followed the method described by Bates et al. (1973). The reaction mixture consisted of 400 µL of plant extract, glacial acetic acid, and acidic ninhydrin (0.14 M ninhydrin prepared in a mixture of 18 mL glacial acetic acid and 12 mL 6 M phosphoric acid). The mixture was briefly mixed and incubated for 1 h at 100 °C. After that, 1 mL of toluene was added, the mixture was briefly mixed, and the upper phase was collected to measure the absorbance at 520 nm. Proline content was calculated using a calibration curve for which a series of known L-proline concentrations (1–500 µM) were prepared, and the results were expressed as µmol proline per gram of fresh weight (µmol g^{-1} FW).

2.6.4. Gene expression analysis

Total RNA isolation was performed by extracting RNA from 40–50 mg of frozen homogenized seedlings using the MagMax™ Plant RNA Isolation Kit. RNA quantification was performed by measuring absorbance, after which cDNA was synthesized from 1 µg of total RNA using 2.5 µM of Oligo(dT)18 primer, 1 mM of dNTPs, 1 × Reaction Buffer, 20 U of RiboLock RNase inhibitor, and 200 U of RevertAid H Minus Reverse Transcriptase in a total volume of 20 µL. The reaction procedure was as follows: 65 °C for 5 min, 42 °C for 1 h and 70 °C for 15 min. The cDNA was diluted and checked for gDNA contamination by standard PCR amplification and agarose electrophoresis of the *ACT3* gene (At3G53750; FW 5′-CTGGCATCATACTTTCTACAATG-3′, REV 5′-CACCACTGAGCACAATGTTAC-3′). Relative quantification of *DMS3* gene expression in control seedlings was performed by qPCR on the MIC qPCR Cycler platform (Bio Molecular Systems) using 1 × GoTaq® qPCR Master Mix reagent, 200 nM of gene-specific primers (At3G49250.1; FW 5′-CGATATGATTAGTGCCCTCCC-3′, REV 5′-GTTCACCTCATCACGGTTTCC-3′), and 10 ng of cDNA in a total reaction volume of 10 µL. The ΔΔCt method was used to calculate relative gene expression (Pfaffl, 2001; Vandesompele et al., 2002), with the *OGIO* gene (At5G51880.1; FW 5′-ATCCAAGAGCAGTTCAAGCAAG-3′, REV 5′-GAGAGCCATACCTTCCACTG-3′) as an endogenous control (Škiljaica et al., 2022). The reaction procedure was as follows: 5 min at 95 °C, followed by 40 cycles at 95 °C for 10 s and 60 °C for 10 s. Specific amplification was confirmed using no-template controls and melting curves (55 °C to 95 °C at 0.5 °C s^{-1}), and C_t values and primer efficiencies were calculated using MIC qPCR Cycler software (Bio Molecular Systems).

2.7. Statistical analysis

Prior to statistical analysis, data were checked for outliers using Tukey's fences with k set to 1.5. The distribution of the continuous data for the measured parameters was assessed using the Shapiro-Wilk W test, while the homogeneity of variances was assessed using the Levene's test. The data were considered normally distributed, and the variances were considered equal if $p > 0.05$. Depending on the number of groups compared, either a Student's *t*-test for independent samples (for two groups) or a two-way ANOVA (for multiple groups) was performed. If the two-way ANOVA revealed significant group differences, a one-way ANOVA followed by Tukey HSD *post hoc* analysis was conducted to determine which groups showed significant differences. The Chi-square test of independence was used to compare the seedling survival percentage between the tested lines. The statistical significance was set at $p \leq 0.05$. To visualize similarities in hormone levels and their metabolites, heatmap and cluster analyses were generated using R software version

4.1.1 with the "*ComplexHeatmap*" package (Gu et al., 2016). The dendrograms were constructed based on Euclidean distance.

3. Results

3.1. DMS3 protein expression in lines with altered DMS3 gene

The first independent line overexpressing *DMS3* gene (*oeDMS3* 6TV6) showed at least a 30-fold higher level of *DMS3* transcripts (endogenous *DMS3* and transgenic *GFP-DMS3*) compared to the wild type, while the second independent line (*oeDMS3* 4TV7) showed a 15-fold increase (Fig. 1a). Conversely, expression of the mutated *DMS3* gene was reduced in the *dms3-1* mutant line. Despite lower *DMS3* transcript levels in the *oeDMS3* 4TV7 line compared to the *oeDMS3* 6TV6, both native and recombinant DMS3 protein accumulated at higher levels in the *oeDMS3* 4TV7 line than in *oeDMS3* 6TV6 (Fig. 1b, c). However, the total amount of DMS3 protein in seedlings, including endogenous DMS3 and transgenic GFP-DMS3, was significantly higher in both overexpressing lines compared to the wild type, 3-fold higher in *oeDMS3* 6TV6 and 8-fold higher in *oeDMS3* 4TV7 (Fig. 1c). Consistent with the protein quantification results, GFP-DMS3 signals visualized by fluorescence microscopy were more intense in the root tissue of *oeDMS3* 4TV7 line (Fig. 1d). However, the *in situ* distribution of the GFP-DMS3 signal in seedling roots was similar in both lines.

3.2. Viability of seedlings after heat stress

To determine the thermosensitivity of *A. thaliana* seedlings with altered *DMS3* expression after a 45- min heat shock at 45 °C, seedlings' viability was assessed during a seven-day recovery period (Fig. 2a). Under control conditions, all lines tested showed 100 % survival (data not shown). However, after heat treatment, the survival percentage of *dms3-1* seedlings decreased significantly compared to *oeDMS3* and wild-type seedlings. The viability of the seedlings was monitored from the

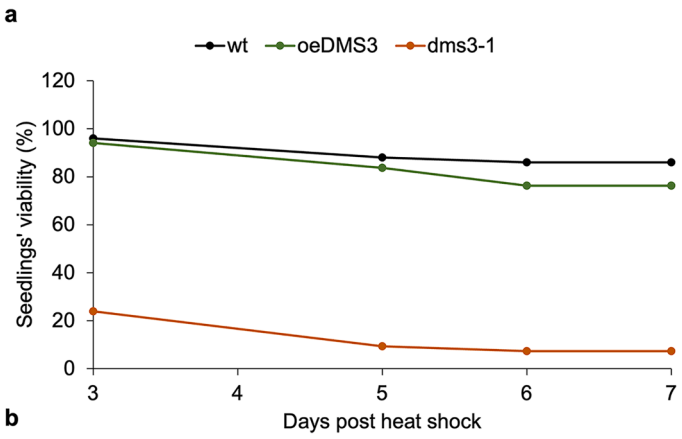

b

	3rd	5th	6th	7th
	Chi-square test statistic (χ^2)			
wt × *oeDMS3*	0.05 ns	0.12 ns	0.75 ns	0.75 ns
wt × *dms3-1*	78.57 ***	77.11 ***	99.66 ***	99.66 ***
oeDMS3 × *dms3-1*	58.18 ***	54.23 ***	83.43 ***	83.43 ***

Fig. 2. Heat shock significantly affected viability of *dms3–1* seedlings. (**a**) The *Arabidopsis thaliana* seedlings overexpressing the *DMS3* gene (*oeDMS3*), with a mutated *DMS3* gene (*dms3-1*) and wild type (wt) were heat-treated at 45 °C for 45 min. The percentage of viable seedlings was assessed during a seven-day recovery period, starting on the third day. Results are expressed as the ratio of surviving seedlings to the total number of seedlings (n = 100) and multiplied by 100 %. (**b**) Statistical analysis of the differences among tested lines was performed using the Chi-square test of independence. Significant differences ($p \leq 0.001$) are marked with asterisks (***).

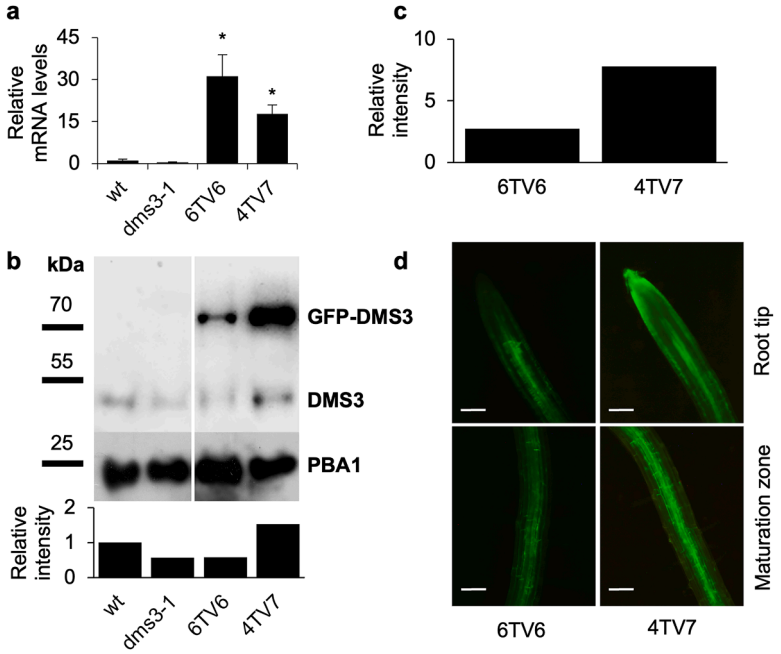

Fig. 1. Two independent transgenic lines accumulated GFP-DMS3 protein. (**a**) Total (endogenous and transgenic) levels of *DMS3* transcript in *Arabidopsis thaliana* wild type (wt), line with a mutated *DMS3* gene (*dms3-1*), and two lines overexpressing the *DMS3* gene (*oeDMS3* 6TV6 and 4TV7). An asterisk (*) indicates a significant difference compared to wt (Student's *t*-test, $p \leq 0.05$). (**b**) Immunodetection of endogenous DMS3 and transgenic GFP-DMS3 protein levels in wt, *dms3-1*, *oeDMS3* 6TV6 and 4TV7. Immunodetection was performed on two biological replicates and a representative membrane is shown. PBA1 protein was used as a loading control. Results of endogenous DMS3 are expressed as relative band intensity compared to wt (=1). (**c**) Endogenous and transgenic DMS3 protein levels, based on immunodetection as shown in (b). (**d**) GFP-DMS3 was visualized in *oeDMS3* 6TV6 and 4TV7 under a fluorescence microscope. Photographed were root tip and maturation zone regions. Scale bars are 100 μm.

third day after treatment. At this point, differences in survival became apparent, and this trend continued until the end of the experiment (Fig. 2b).

3.3. Morphology, biomass and chlorophyll fluorescence of lines with altered DMS3

Our further aim in characterizing the *DMS3*-altered lines was to expose the plants to moderate heat stress, *i.e.*, 40 °C for 6 h, as this type of treatment better reflects the temperature fluctuations to which the plants are likely to be exposed in their natural environment. High-

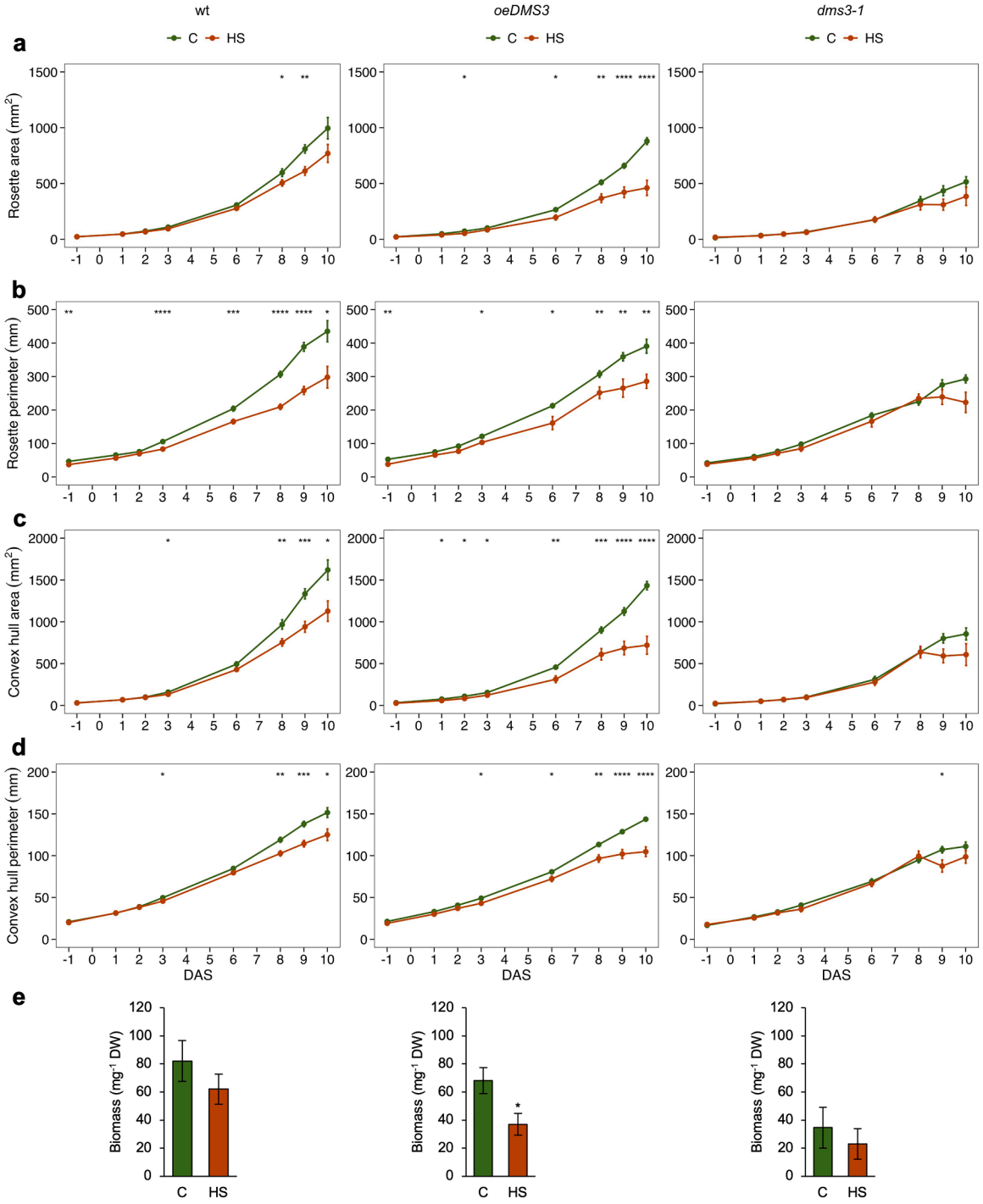

Fig. 3. Moderate heat stress caused the strongest morphological reduction in the *DMS3*-overexpressing line. The *Arabidopsis thaliana* plants overexpressing the *DMS3* gene (*oeDMS3*), with a mutated *DMS3* gene (*dms3-1*) and wild type (wt) were either kept under control conditions (C) or exposed to heat stress at 40 °C at the two-rosette leaf stage (HS). Four morphological traits were analyzed: (**a**) rosette area, (**b**) rosette perimeter, (**c**) convex hull area and (**d**) convex hull perimeter. Data are presented as means ± standard error of at least 20 biological replicates. (**e**) Biomass is given as mean ± standard error of 6–7 biological replicates. Statistical significance was determined using Student's *t*-test, with significant differences indicated as follows: * $p \leq 0.05$, ** $p \leq 0.01$, *** $p \leq 0.001$, and **** $p \leq 0.0001$. DAS – day after heat stress.

throughput phenotyping revealed that heat stress significantly affected the morphological traits of *A. thaliana* plants overexpressing *DMS3* gene (*oeDMS3*) and wild type (Fig. 3). This was reflected in a reduction of all analyzed morphological traits compared to the respective controls on the last day of the experiment, *i.e.*, 10 days after heat treatment (Fig. 3a-d). The heat-treated *dms3-1* plants showed no significant changes compared to the control plants. However, they showed about 1.4-fold lower values for rosette area, perimeter and convex hull area than control plants. Reduced morphological traits in heat-treated *oeDMS3* plants correlated with lower biomass, as these had showed significantly lower biomass than the control plants (Fig. 3e). Although the changes in heat-treated *dms3-1* and wild-type plants were not significant, it is worth noting that these plants had 1.3- and 1.5-fold lower biomass, respectively, than the corresponding controls. Interestingly, the rosette area proved to be more sensitive to heat stress compared to the perimeter-related parameters as the first significant changes were observed within one day after heat treatment. In particular, *oeDMS3* plants showed increased sensitivity compared to wild-type and *dms3-1* plants, with rosette area and convex hull area significantly decreasing as early as 24 h after treatment. When comparing the effects of *DMS3* expression alone, the *dms3-1* plants showed lower growth under control conditions, as indicated by the smallest rosette area and lowest biomass compared to the *oeDMS3* line and the wild type (Suppl. Fig. 3a, b). The measurement of the maximum quantum yield of photosystem II (F_V/F_M) showed that *dms3-1* plants had the lowest values under both stress and control conditions, compared to the *oeDMS3* line and the wild-type plants (Suppl. Fig. 4a, b).

3.4. Hormonal changes induced by heat and modifications in DMS3 expression

Hormonal profiling revealed that heat stress had long-term effects on hormone levels, as evidenced by significant differences in some hormones and their metabolites seven days after treatment (Fig. 4). In wild-type plants, heat stress led to significant upregulation of cytokinin metabolism, marked by higher levels of dihydrozeatin (DHZ) types, ribosides, and total cytokinins. The DHZ types included dihydrozeatin riboside (DHZR) and dihydrozeatin 7-glucoside (DHZ7G), while the total amount of cytokinins included the sum of bases, ribosides, O-glucosides and N-glucosides. The increased levels of DHZ types were likely due to significantly increased DHZ7G content, and the rise in total cytokinin levels was likely due to higher ribosides level (Suppl. Table 1). Although these changes were not statistically significant in heat-treated *dms3-1* plants, this line exhibited even more pronounced changes in cytokinin content than the wild type, primarily due to notably increased riboside levels (Suppl. Table 1). Analysis of the jasmonates revealed contrasting trends between plants with altered *DMS3* expression and the wild type. In the heat-treated wild type, the levels of the precursor cis-(+)-12-oxo-phytodienoic acid (cisOPDA) and the bioactive jasmonic acid (JA) and jasmonoyl-L-isoleucine (JA-Ile) were significantly lower compared to the control. In contrast, no changes in jasmonate metabolism in response to heat stress were observed in lines with altered *DMS3* expression. Under control conditions, these plants showed higher cisOPDA levels and lower JA and JA-Ile levels compared to wild type. As far as abscisic acid (ABA) is concerned, reduced levels were observed in all treated plants. However, only the *dms3-1* line and the wild type showed a significant reduction in ABA levels. Regarding auxin metabolism, the precursor anthranilate (ANT) and the catabolite 2-oxo-IAA (oxIAA) and conjugate IAA-aspartate (IAA-Asp) were significantly increased in heat-treated *dms3-1* plants. Conversely, heat-treated wild-type plants showed higher levels of the precursor indole-3-acetamide (IAM), but lower levels of the bioactive indole-3-acetic acid (IAA). The cluster analysis showed that the *DMS3* expression significantly influenced hormone profiles. Plants with altered *DMS3* expression (*oeDMS3, dms3-1*) showed more similar hormone profiles and differed from wild-type plants. This pattern was evident both when comparing control plants alone (Suppl. Fig. 5) and when including heat-treated and control plants in the analysis (Fig. 4).

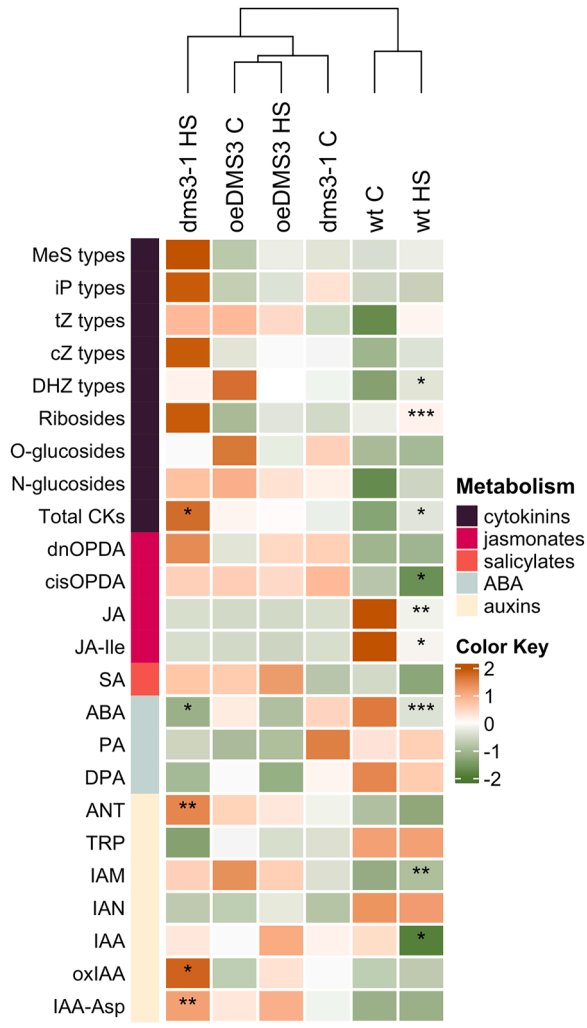

Fig. 4. Cluster analysis revealed that both *DMS3* expression and moderate heat stress affect the plant hormone profile. The *Arabidopsis thaliana* plants overexpressing the *DMS3* gene (*oeDMS3*), with a mutated *DMS3* gene (*dms3-1*) and wild-type (wt) were either kept under control conditions (C) or exposed to heat stress at 40 °C at the two-rosette leaf stage (HS). Hormone are categorized into five different groups: cytokinins (MeS – unbound methylthiolated cytokinins, iP – N^6-(Δ^2-isopentenyl)-adenine, tZ – trans-zeatin, cZ – cis-zeatin, DHZ – dihydrozeatin, ribosides, O-glucosides, N-glucosides), jasmonates (dnOPDA – dinor-12-oxo-phytodienoic acid, cisOPDA – cis-(+)-12-oxo-phytodienoic acid, JA – jasmonic acid, JA-Ile – jasmonoyl-L-isoleucine), salicylates (SA – salicylic acid), ABA (ABA – abscisic acid, PA – phaseic acid, DPA – dihydrophaseic acid), and auxins (ANT – anthranilate, TRP – tryptophan, IAM – indole-3-acetamide, IAN – indole-3-acetonitrile, IAA – indole-3-acetic acid, oxIAA – 2-oxo-IAA, IAA-Asp – IAA-aspartate). Color intensities represent normalized hormone levels, with brown indicating higher abundance and green indicating lower abundance relative to the mean, based on three biological replicates. Statistical significance between treated *A. thaliana* lines and corresponding controls was determined using Student's *t*-test, with significant differences indicated as follows: * $p \leq 0.05$, ** $p \leq 0.01$, *** $p \leq 0.001$, and **** $p \leq 0.0001$. Cluster analysis was performed using Euclidean distance.

3.5. Heat stress-induced changes in DMS3 protein stability and localization in roots

Further analyzes were carried out in an *in vitro* system. Therefore, plants were exposed to 37 °C rather than 40 °C to account for the higher humidity and lower evaporative cooling typically associated with *in vitro*

conditions. To investigate the stability and abundance of DMS3 protein at elevated temperature, we subjected *oeDMS3* seedlings to 37 °C for 24 h and analyzed them immediately after treatment. The *oeDMS3* 4TV7 transgenic line was used for this analysis. The GFP-DMS3 signal was visualized in the meristematic and differentiation zones of the root, with the strongest signals observed in the root tip epidermis, columella, and lateral root cap. It was also found that under control conditions (24 °C), the GFP-DMS3 signal was abundant (Fig. 5a). However, after heat treatment at 37 °C, signals in root tips decreased. In the differentiation zone, GFP-DMS3 protein signal accumulated within cortex cells (Fig. 5b). Interestingly, accumulation intensified at 37 °C in the epidermis region, showing that heat stress significantly affected the stability and localization of the GFP-DMS3 recombinant protein in the root tissue.

3.6. Heat-induced changes in photosynthetic performance

To evaluate the effects of *DMS3* expression and heat stress on photosynthetic performance, plants were exposed to 37 °C for 6 h. In plants with altered *DMS3* gene expression, heat treatment had a significant effect ($F = 13.69$, $p \leq 0.01$) on the F_V/F_M. Immediately after heat exposure a significantly lower F_V/F_M was measured in treated *dms3-1* and *oeDMS3* seedlings while there was no effect on wild-type seedlings (Table 1). After 24-h recovery, there was a significant effect of heat treatment ($F = 3.34$, $p \leq 0.05$) and *DMS3* expression ($F = 3.72$, $p \leq 0.05$). Higher F_V/F_M was observed in treated wild-type seedlings (REC) compared to control seedlings (C-REC). Comparison of lines with altered *DMS3* expression showed that control *oeDMS3* and *dms3-1* seedlings had higher F_V/F_M than control wild-type seedlings.

The absorption-based performance index (PI_{ABS}) measured immediately after treatment was also significantly affected by heat ($F = 10.94$, $p \leq 0.01$). Lower PI_{ABS} was measured in treated *dms3-1* seedlings (HS) than in control seedlings (C-HS) (Table 1). Although the changes in the treated wild-type seedlings (HS) were not statistically significant, it is worth noting that PI_{ABS} decreased 1.35-fold compared to the corresponding control (C-HS). For seedlings analyzed after recovery period, two-way ANOVA showed a significant effect of treatment ($F = 3.91$, $p \leq 0.05$) and *DMS3* expression ($F = 4.23$, $p \leq 0.05$). Similar to seedlings analyzed immediately after treatment, lower PI_{ABS} was measured in treated *dms3-1* seedlings (REC). Comparison of lines with altered *DMS3* expression showed significantly higher levels of PI_{ABS} in control *dms3-1* and *oeDMS3* seedlings (C-REC) compared to the wild type.

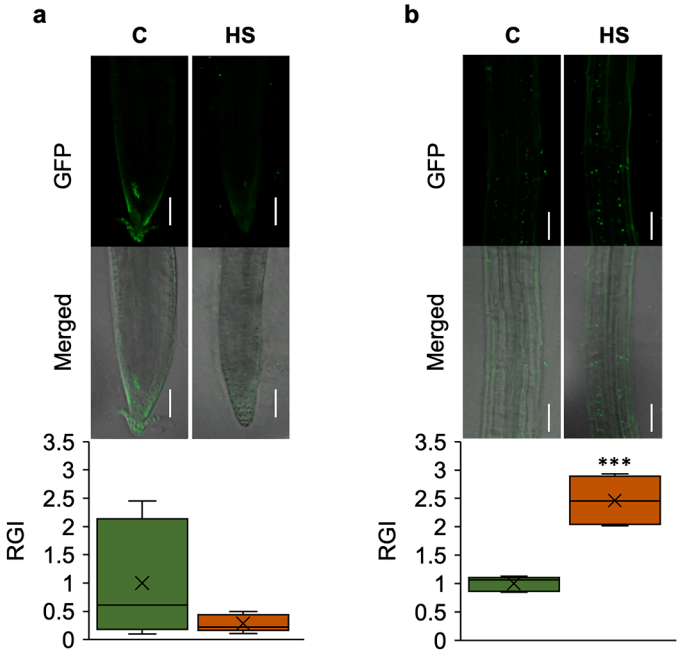

Fig. 5. The stability and localization of the recombinant GFP-DMS3 protein in root tissue was affected by heat stress. The *Arabidopsis thaliana* seedlings overexpressing *DMS3* gene were exposed to 37 °C for 24 h (HS) and compared to control (C) grown at 24 °C. Confocal microscopy was used to capture images of seedling roots in (**a**) meristematic and (**b**) differentiation zones. Both fluorescent and merged (bright field and GFP signal) images are shown. Relative GFP intensities (RGI) were normalized to control values. Data are presented as means and medians of five to six biological replicates, with whiskers showing the range of the data set. Statistical analysis was performed with Student's *t*-test, and significant differences ($p \leq 0.001$) are marked with asterisks (***). Scale bars represent 50 μm.

In seedlings sampled immediately after heat treatment, only the *DMS3* expression influenced specific energy fluxes – absorption (ABS/RC; $F = 10.34$, $p \leq 0.01$), trapping (TR_0/RC; $F = 14.1$, $p \leq 0.001$) and electron transport (ET_0/RC; $F = 5.71$, $p \leq 0.01$) per active photosystem II reaction center. Consequently, only treated *dms3*-1 and *oeDMS3* seedlings (HS) had lower values for ABS/RC and TR_0/RC compared to treated wild-type seedlings (Table 1). In addition, treated *dms3-1* seedlings (HS) had lower ET_0/RC than the wild type. On the other hand, in *dms3-1* seedlings treatment caused a significant increase ($F = 7.09$, $p \leq 0.01$) of dissipation of energy as heat (DI_0/RC) compared to the respective control. After 24 h of recovery, all specific energy fluxes were influenced by treatment (ABS/RC – $F = 18.99$, $p \leq 0.0001$; TR_0/RC – $F = 30.18$, $p \leq 0.0001$; ET_0/RC – $F = 45.38$, $p \leq 0.0001$; DI_0/RC – $F = 7.29$, $p \leq 0.01$) and *DMS3* expression (ABS/RC – $F = 8.92$, $p \leq 0.01$; TR_0/RC – $F = 11.96$, $p \leq 0.01$; ET_0/RC – $F = 6.89$, $p \leq 0.01$; DI_0/RC – $F = 11.05$, $p \leq 0.01$). A decrease in ABS/RC was observed in treated *dms3-1* and wild-type seedlings (REC) compared to the respective controls (C-REC) (Table 1). A significant reduction in TR_0/RC and ET_0/RC was noticed in all treated seedlings (REC), regardless of the line. In contrast, DI_0/RC increased significantly only in treated wild-type seedlings. Comparison of lines with altered *DMS3* expression showed that control *oeDMS3* seedlings (C-REC) had lower ABS/RC, TR_0/RC, and ET_0/RC than the wild type. In addition, treated *dms3-1* and *oeDMS3* seedlings (REC) had lower ABS/RC and TR_0/RC than wild-type seedlings. In treated *dms3-1* seedlings, ET_0/RC was significantly lower compared to the wild type. DI_0/RC analysis showed that control *dms3-1* and *oeDMS3* seedlings (C-REC) had lower values than wild-type seedlings.

The density of active reaction centers per excited leaf cross-section (RC/CS_0) measured immediately after heat treatment was significantly affected by the interaction of treatment and *DMS3* expression ($F = 3.66$, $p \leq 0.05$). Treated *dms3-1* seedlings (HS) had a lower RC/CS_0 value compared to the corresponding control (C-HS) (Table 1). At the same time, treated *oeDMS3* seedlings had higher RC/CS_0 than control seedlings. Comparison of lines with altered *DMS3* expression showed that treated *dms3-1* seedlings (HS) had the lowest RC/CS_0 compared to the *oeDMS3* seedlings and wild type. Moreover, treated *oeDMS3* seedlings had significantly higher RC/CS_0 than the wild type. After recovery, there was no significant effect of treatment, *DMS3* expression, or their interaction on the RC/CS_0 parameter.

3.7. Impact of heat stress and DMS3 expression on RuBisCO, HSP90 and HSP70 protein levels

Exposure to 37 °C for 6 h did not significantly affect the expression of the large subunit of the RuBisCO protein (rbcL). A notable decrease (about 1.5-fold) in rbcL expression was observed only in treated *oeDMS3* seedlings (HS) immediately after exposure to elevated temperature compared to the corresponding control (C-HS) (Fig. 6a, Suppl. Fig. 6). However, after 24 h, no notable difference in rbcL expression was observed between the control (C-REC) and the treated seedlings (REC), regardless of *DMS3* expression. Comparison of lines with altered *DMS3* expression under control conditions revealed that *dms3-1* seedlings sampled at both time points had approximately 1.5-fold lower rbcL expression than *oeDMS3* and wild-type seedlings.

Table 1
Seedlings with a mutated *DMS3* gene showed the highest sensitivity of the photosynthetic apparatus to moderate heat stress. Maximum quantum yield of PSII (F_V/F_M), absorption-based performance index (PI_{ABS}), specific energy fluxes – absorption (ABS/RC), trapping (TR_0/RC), electron transport (ET_0/RC), and dissipation of energy as heat (DI_0/RC) per active PSII reaction center (RC), and the density of active reaction centers per excited leaf cross-section (RC/CS_0) were measured in *Arabidopsis thaliana* seedlings overexpressing the *DMS3* gene (*oeDMS3*), with a mutated *DMS3* gene (*dms3-1*) and wild type (wt). Seedlings were analyzed at two time points: immediately after exposure to 37 °C for 6 h (HS) and after a 24-h recovery period at 24 °C (REC). Control groups (C-HS and C-REC) of each line were grown at 24 °C throughout the experiment. Results are expressed as the mean of five biological replicates ± standard error. The response of control and treated plants (C-HS and HS, or C-REC and REC) within each line (wt, *oeDMS3*, or *dms3-1*) was analyzed using Student's *t*-test. Significant differences ($p \leq 0.05$) between C-HS and HS are marked with an asterisk (*), and between C-REC and REC with a hash mark (#). Response of control (C-HS or C-REC) and treated (HS or REC) plants of different lines (wt, *oeDMS3*, and *dms3-1*) was analyzed using one-way ANOVA followed by Tukey HSD test. Significant differences ($p \leq 0.05$) are marked with different capital letters.

DMS3 EXPRESSION	GROUP	F_V/F_M	PI_{ABS}	ABS/RC	TR_0/RC	ET_0/RC	DI_0/RC	RC/CS_0
wt	C-HS	0.75 ± 0.01 A	1.70 ± 0.28 A	2.99 ± 0.11 A	2.24 ± 0.05 A	1.35 ± 0.04 A	0.75 ± 0.07 A	4939 ± 435 A
	HS	0.74 ± 0.00 A	1.27 ± 0.06 A	3.05 ± 0.03 A	2.26 ± 0.03 A	1.29 ± 0.02 A	0.78 ± 0.02 A	5236 ± 162 B
	C-REC	0.74 ± 0.01 B	1.28 ± 0.05 B	3.17 ± 0.04 A	2.34 ± 0.03 A	1.38 ± 0.02 A	0.83 ± 0.02 A	6084 ± 322 A
	REC	0.76 ± 0.01 A#	1.42 ± 0.15 A	2.87 ± 0.06 A#	2.18 ± 0.03 A#	1.21 ± 0.05 A#	0.68 ± 0.04 A#	5189 ± 295 A
oeDMS3	C-HS	0.78 ± 0.00 A	1.90 ± 0.11 A	2.70 ± 0.05 A	2.10 ± 0.05 A	1.24 ± 0.03 A	0.60 ± 0.01 A	5200 ± 227 A
	HS	0.75 ± 0.01 A*	1.54 ± 0.15 A	2.78 ± 0.08 B	2.09 ± 0.04 B	1.21 ± 0.03 AB	0.69 ± 0.04 A	5941 ± 90 A*
	C-REC	0.77 ± 0.01 A	1.78 ± 0.19 A	2.81 ± 0.08 B	2.16 ± 0.04 B	1.28 ± 0.03 B	0.65 ± 0.04 B	5780 ± 160 A
	REC	0.77 ± 0.01 A	1.72 ± 0.17 A	2.62 ± 0.06 B	2.01 ± 0.05 B#	1.15 ± 0.04 AB#	0.61 ± 0.02 A	5175 ± 233 A
dms3–1	C-HS	0.78 ± 0.00 A	2.06 ± 0.09 A	2.70 ± 0.03 A	2.09 ± 0.02 A	1.22 ± 0.06 A	0.60 ± 0.01 A	5406 ± 52 A
	HS	0.73 ± 0.01 A*	1.30 ± 0.24 A*	2.76 ± 0.06 B	2.01 ± 0.04 B	1.11 ± 0.07 B	0.75 ± 0.04 A*	4774 ± 216 C*
	C-REC	0.77 ± 0.00 A	1.83 ± 0.07 A	2.91 ± 0.12 AB	2.20 ± 0.05 AB	1.29 ± 0.03 AB	0.64 ± 0.02 B	5292 ± 420 A
	REC	0.76 ± 0.01 A	1.42 ± 0.13 A#	2.60 ± 0.04 B#	1.97 ± 0.02 B#	1.05 ± 0.03 B#	0.62 ± 0.03 A	4682 ± 214 A

Heat treatment resulted in a remarkable increase in HSP90 protein expression in treated *dms3-1* seedlings (HS) by 10.3-fold and in *oeDMS3* seedlings by 2.5-fold compared to the corresponding controls (C-HS), whereas the wild type showed only a modest increase of 1.3-fold (Fig. 6b, Suppl. Fig. 6). HSP90 expression remained elevated after recovery (REC) compared to control seedlings, with a 2.7-fold increase in the *dms3-1* line, a 1.6-fold increase in the *oeDMS3* line and a 1.8-fold increase in the wild type. It is noteworthy that the control seedlings of the *dms3-1* line sampled at both time points showed lower HSP90 expression than the wild-type seedlings. Specifically, HSP90 levels in *dms3-1* were lower 4.3-fold in C-HS and 3.3-fold in C-REC compared to wild type. In contrast to HSP90, HSP70 expression did not increase in heat-treated *oeDMS3* or *dms3-1* seedlings (HS) immediately after stress, whereas a 1.4-fold increase was observed in the wild type under the same conditions (Fig. 6c, Suppl. Fig. 6). After a 24-h recovery period, HSP70 levels returned to baseline in the wild-type seedlings, whereas a 1.5-fold increase was observed in the *dms3-1* seedlings (REC) compared to the corresponding control (C-REC). Similar to HSP90, the *dms3-1* line showed approximately 2-fold lower baseline HSP70 expression at both sampling points (C-HS and C-REC) compared to the wild type.

3.8. Activation of the antioxidant system in response to heat treatment

Exposure to 37 °C for 6 h affected antioxidant activity. In lines with altered *DMS3* expression, SOD activity was significantly affected only by the interaction of treatment and *DMS3* expression ($F = 5.49$, $p \leq 0.05$). On the other hand, analysis of G-POD activity showed a dependence on heat treatment ($F = 5.20$, $p \leq 0.05$), *DMS3* expression ($F = 15.05$, $p \leq 0.0001$), and their interaction ($F = 14.46$, $p \leq 0.0001$). The activity of both enzymes significantly increased in treated *oeDMS3* seedlings (HS) compared to control seedlings (C-HS) (Fig. 7a, b). In contrast, G-POD activity decreased 1.98-fold in treated *dms3-1* seedlings. Comparison of lines with altered *DMS3* expression showed significantly lower G-POD activity in control *oeDMS3* seedlings (C-HS) than in the wild type. On the contrary, treated *dms3-1* seedlings (HS) had significantly lower G-POD activity than the *oeDMS3* line and the wild type. Analysis of SOD activity showed higher enzyme activity in control *dms3-1* seedlings (C-HS) compared to the *oeDMS3* line (HS). APX activity measured immediately after treatment was affected by treatment alone ($F = 11.95$, $p \leq 0.01$), while CAT activity was affected by treatment ($F = 28.95$, $p \leq 0.0001$) and *DMS3* expression ($F = 9.83$, $p \leq 0.01$). The activity of both enzymes significantly increased in treated wild-type seedlings (HS) (Fig. 7c, d). In addition, significantly higher APX activity was observed in treated *oeDMS3* seedlings, while CAT activity was significantly higher in treated *dms3-1* seedlings. Although the change was not statistically significant, CAT activity increased 1.3-fold in treated *oeDMS3* seedlings compared to control seedlings. Regarding the comparison of lines with altered *DMS3* expression, treated *dms3-1* seedlings (HS) had significantly higher CAT activity than the corresponding *oeDMS3* and wild-type seedlings.

After 24 h of recovery, SOD activity was significantly dependent on treatment ($F = 8.90$, $p \leq 0.01$) and *DMS3* expression ($F = 6.04$, $p \leq 0.01$). Only treated *oeDMS3* seedlings (REC) were found to have significantly lower SOD activity compared to control seedlings (Fig. 7a). Comparison of lines with altered *DMS3* expression revealed that treated *dms3-1* seedlings (REC) had significantly higher SOD activity than treated *oeDMS3* seedlings. Regarding G-POD activity, only *DMS3* expression significantly influenced activity ($F = 5.11$, $p \leq 0.05$). Nevertheless, G-POD activity in treated *dms3-1* seedlings (REC) decreased 1.3-fold compared to control values (Fig. 7b). Comparison of lines with altered *DMS3* expression showed significantly higher G-POD activity in control (C-REC) and treated *dms3-1* seedlings (REC) compared to *oeDMS3* and wild-type seedlings, respectively. APX activity showed a significant dependence on treatment ($F = 9.45$, $p \leq 0.01$), *DMS3* expression ($F = 5.06$, $p \leq 0.05$), and their interaction ($F = 6.41$, $p \leq 0.01$). In contrast, CAT activity was significantly affected only by treatment ($F = 6.70$, $p \leq 0.01$). The activity of both enzymes increased significantly in treated wild-type seedlings (REC) (Fig. 7c, d). Although the difference was not statistically significant, CAT activity increased 1.3-fold in treated *dms3-1* seedlings (REC) compared to control seedlings. When *DMS3* expression was taken into account, significantly higher APX activity was observed in the *oeDMS3* and *dms3-1* control seedlings (C-REC) compared to the wild type.

3.9. Effect of heat and altered DMS3 expression on proline content

Like the antioxidant activity, the proline content was also influenced by heat treatment at 37 °C for 6 h. Accordingly, proline content measured immediately after treatment in lines with altered *DMS3* expression showed a dependence on heat treatment ($F = 231.11$, $p \leq 0.0001$), *DMS3* expression ($F = 17.84$, $p \leq 0.0001$), and their interaction ($F = 14.88$, $p \leq 0.0001$). A significantly lower proline content was measured in all treated seedlings (HS) than in the corresponding controls (C-HS) (Fig. 8). Comparison of lines with altered *DMS3* expression showed that control *oeDMS3* seedlings (C-HS) had significantly lower

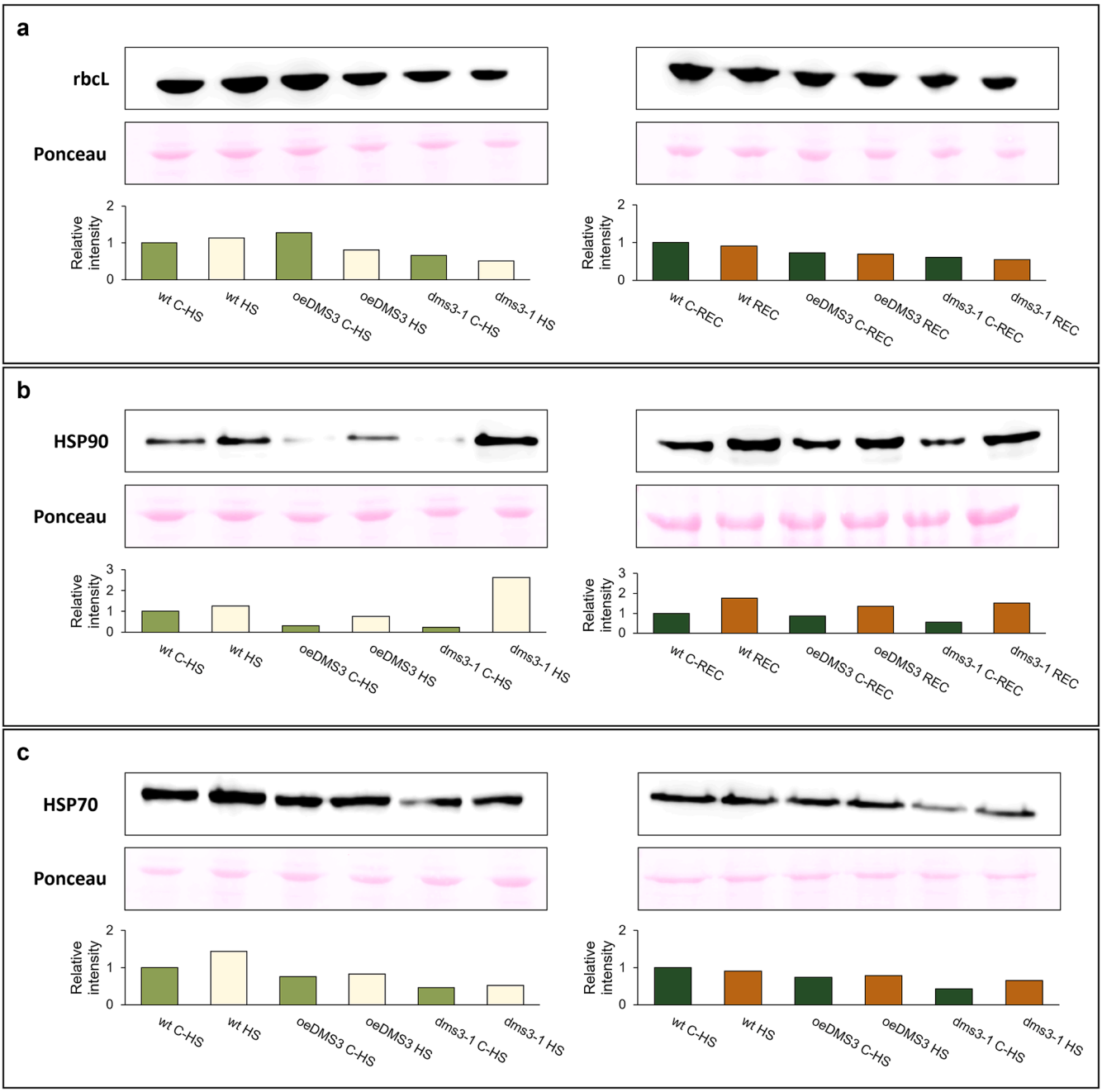

Fig. 6. Seedlings with a mutated *DMS3* gene showed lower expression of RuBisCO large subunit (rbcL), HSP90 and HSP70 proteins than wild type. (**a**) rbcL, (**b**) HSP90 and (**c**) HSP70 proteins were immunoblotted in *Arabidopsis thaliana* seedlings overexpressing the *DMS3* gene (*oeDMS3*), with a mutated *DMS3* gene (*dms3-1*) and wild type (wt). Seedlings were sampled at two time points: immediately after exposure to 37 °C for 6 h (HS) and after a 24-h recovery period at 24 °C (REC). Control groups (C-HS and C-REC) of each line were grown at 24 °C throughout the experiment. Ponceau staining of the membranes was used as a loading control. Results are expressed as relative band intensity compared to wt C-HS or wt C-REC (=1). Immunodetection was performed on two biological replicates, and one representative membrane per protein is shown.

proline content than *dms3-1* and wild-type seedlings.

After recovery, there were also significant effects of heat treatment ($F = 7.81$, $p \leq 0.01$), *DMS3* expression ($F = 14.24$, $p \leq 0.001$), and their interaction ($F = 3.52$, $p \leq 0.05$). Significantly higher proline content was observed only in treated *dms3-1* seedlings (REC) (Fig. 8). Analysis of lines with *DMS3* expression revealed that control *oeDMS3* and *dms3-1* seedlings (C-REC) had significantly lower proline content compared to the wild type. In addition, treated *oeDMS3* seedlings (REC) had significantly lower proline content than the *dms3-1* line and the wild type.

4. Discussion

4.1. DMS3-altered lines show a stronger reduction in morphological parameters in response to heat stress

Root and shoot growth inhibition, leaf discoloration, accelerated senescence and abscission are common indicators of heat stress (Fahad et al., 2017; Rodríguez et al., 2005). In line with these findings, our phenotyping experiment showed that all treated plants exhibited signs of heat stress, such as inhibition of rosette growth and reduced biomass. However, at the end of the experiment, both *DMS3*-altered lines

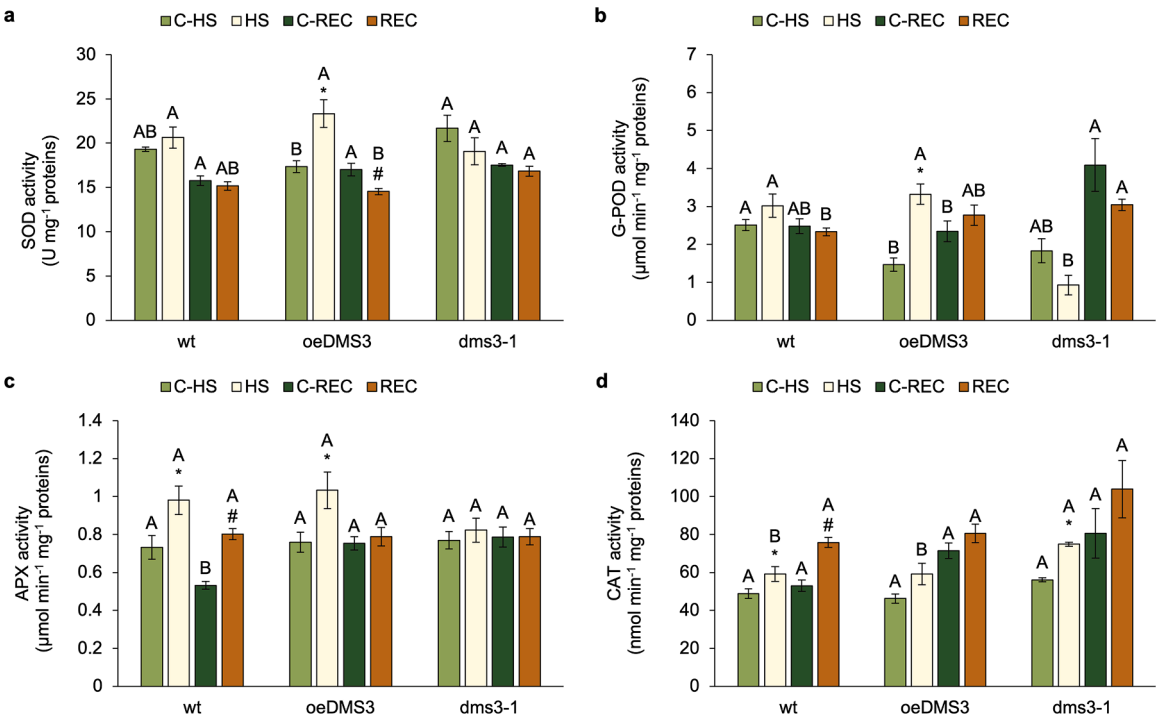

Fig. 7. The *DMS3*-overexpressing line showed partial activation of antioxidant enzymes after exposure to moderate heat stress. Activity of (**a**) superoxide dismutase (SOD), (**b**) guaiacol peroxidase (G-POD), (**c**) ascorbate peroxidase (APX), and (**d**) catalase (CAT) was measured in *Arabidopsis thaliana* seedlings overexpressing the *DMS3* gene (*oeDMS3*), with a mutated *DMS3* gene (*dms3-1*) and wild type (wt). Seedlings were sampled at two time points: immediately after exposure to 37 °C for 6 h (HS) and after a 24-h recovery period at 24 °C (REC). Control groups (C-HS and C-REC) of each line were grown at 24 °C throughout the experiment. Results are expressed as the mean of five biological replicates ± standard error. The response of control and treated plants (C-HS and HS, or C-REC and REC) within each line (wt, *oeDMS3*, or *dms3-1*) was analyzed using Student's *t*-test. Significant differences ($p \leq 0.05$) between C-HS and HS are marked with an asterisk (*), and between C-REC and REC with a hash mark (#). Response of control (C-HS or C-REC) and treated (HS or REC) plants of different lines (wt, *oeDMS3*, and *dms3-1*) was analyzed using one-way ANOVA followed by Tukey HSD test. Significant differences ($p \leq 0.05$) are marked with different capital letters.

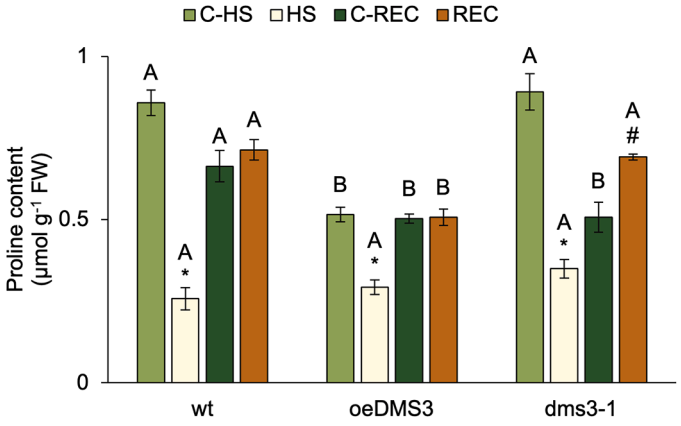

Fig. 8. Only the line with a mutated *DMS3* gene had an increased proline content after recovery from moderate heat stress. Proline content was measured in *Arabidopsis thaliana* seedlings overexpressing the *DMS3* gene (*oeDMS3*), with a mutated *DMS3* gene (*dms3-1*) and wild type (wt). Seedlings were sampled at two time points: immediately after exposure to 37 °C for 6 h (HS) and after a 24-h recovery period at 24 °C (REC). Control groups (C-HS and C-REC) of each line were grown at 24 °C throughout the experiment. Results are expressed as the mean of five biological replicates ± standard error. The response of control and treated plants (C-HS and HS, or C-REC and REC) within each line (wt, *oeDMS3*, or *dms3-1*) was analyzed using Student's *t*-test. Significant differences ($p \leq 0.05$) between C-HS and HS are marked with an asterisk (*), and between C-REC and REC with a hash mark (#). Response of control (C-HS or C-REC) and treated (HS or REC) plants of different lines (wt, *oeDMS3*, and *dms3-1*) was analyzed using one-way ANOVA followed by Tukey HSD test. Significant differences ($p \leq 0.05$) are marked with different capital letters.

(*oeDMS3* and *dms3-1*) showed a greater decrease in morphological parameters than the wild type, indicating the role of DMS3 in the heat response. Plants in which the RdDM signaling pathway is disrupted often show increased sensitivity to abiotic and biotic stress. For example, exposure of *A. thaliana* mutants with silenced RdDM components to 42 °C for 24 h causes lower survival compared to the wild type (Popova et al., 2013). Similarly, tobacco plants (*Nicotiana benthamiana*) with impaired RdDM show higher susceptibility to viral infection compared to plants with functional RdDM, resulting in more severe infection symptoms, higher accumulation of viral DNA and pronounced cellular damage (Zhong et al., 2017). The *oeDMS3* line showed a comparable and, in some cases, even more pronounced decline in morphological parameters than the *dms3-1* mutant, but it is important to note that *dms3-1* line showed lower growth under control conditions, compared to the *oeDMS3* line and the wild type. This suggests that both non-functional and excessive levels of DMS3 can impair RdDM-related functions, indicating a dose-dependent role of DMS3 in regulating heat stress responses. This interpretation is supported by the findings of Zhong et al. (2019), who showed that the anaphase-promoting complex/cyclosome (APC/C) regulates cellular DMS3 levels and that its disruption leads to increased DMS3 levels, decreased polymerase (Pol) V recruitment and impaired RdDM function. Thus, the disrupted RdDM mechanism in *oeDMS3* plants likely impairs the response to heat stress, similar to the reduced thermotolerance and stunted growth observed in the heat-treated *dms3-1* line. Furthermore, our findings on the stability and altered localization of the DMS3 protein in root tissue under heat stress suggest a possible role in regulating root growth, which is consistent with findings linking methylation and root development under heat stress (Hossain et al., 2017).

4.2. Heat stress and DMS3 expression influence the hormonal profile

Changes in plant hormone metabolism are closely linked to the response to heat stress (Jha et al., 2022; Peleg and Blumwald, 2011; Prerostova and Vankova, 2023). Our analysis revealed complex hormonal adjustments, particularly in the *dms3-1* line and wild type. Levels of JA and its bioactive form JA-Ile varied in all analyzed lines under both heat stress and control conditions. As reported by Xu et al. (2016), JA concentrations usually show a sharp increase within the first 2 h of heat stress before dropping to control levels. This may explain why JA and JA-Ile levels were reduced seven days after treatment, as observed in our study. Moreover, both the *dms3-1* and *oeDMS3* control plants had lower JA and JA-Ile levels than the wild type (Suppl. Fig. 5), possibly contributing to their lower thermotolerance. The reduced JA response suggests a possible disruption of JA-mediated defense mechanisms, especially since JA-Ile plays a central role in enhancing stress tolerance (Wang et al., 2023). The *dms3-1* line also exhibited higher levels of dnOPDA and cisOPDA, further supporting the hypothesis of impaired JA metabolism affecting stress resistance. Hazman et al. (2015) reported that plants with lower levels of OPDA, a biologically active precursor of JA, showed improved antioxidant properties compared to plants with elevated OPDA levels. These results support the hypothesis that more impaired JA metabolism in the *dms3-1* line may cause the lower thermotolerance of this line compared to the *oeDMS3* line and the wild type.

ABA, another important stress hormone, decreased in all treated lines, which is consistent with Li et al. (2020) who reported early increase of ABA levels during heat stress but decrease during the recovery phase. This trend suggests that the plants in our study began to acclimatize to the heat treatment within seven days. The decrease in ABA levels could also be a sign of a shift towards a dominance of other growth hormones, such as auxin and cytokinin signaling (Jha et al., 2022; Prerostova and Vankova, 2023). IAA content was significantly reduced in the heat-treated wild type, while the *dms3-1* line accumulated inactive auxin metabolites (oxIAA and IAA-Asp). Sakata et al. (2010) and Song et al. (2019) have shown that auxin biosynthesis is downregulated in response to elevated temperatures, which can negatively impact important growth processes such as cell elongation and lateral root formation and could explain the growth inhibition of our heat-treated plants. Intriguingly, our results also suggested that the wild type and the *dms3-1* line have different strategies for auxin metabolism under heat stress. While the wild type downregulated the production of active auxin in response to heat stress, the *dms3-1* mutant accumulated inactive auxin metabolites. This observation suggests a possible role for the RdDM mechanism in regulating auxin homeostasis under heat stress conditions.

The cytokinin content was slightly increased in the heat-treated wild-type plants, while the *dms3-1* line showed a more prominent increase. In contrast to decreased cytokinin content, which is usually detected after exposure to severe unfavourable conditions, under moderate stress cytokinins play a role in maintaining plant growth, and their content may vary depending on the plant organ or tissue as well as the type and duration of stress (Dobrá et al., 2015; Pavlů et al., 2018; Skalák et al., 2016; Veselov et al., 2017). Despite the increased content of endogenous cytokinins, the *dms3-1* line showed lower thermotolerance. Considering types and forms of cytokinins detected in this line, it was found that after heat stress they were predominantly present in the form of ribosides (Suppl. Table 1; Suppl. Fig. 5). According to the study by Romanov and Schmülling (2022), ribosides are an important cellular source of active cytokinins, but they have no cytokinin activity. Moreover, remarkable differences in cytokinin riboside content between three heat-stressed plant lines indicated a possible involvement of RdDM mechanisms in the expression of the genes responsible for the conversion between active cytokinins free bases and ribosides. In addition, the impaired metabolism of other hormones, such as jasmonates and the accumulation of inactive auxin metabolites might be the reason of the lower thermotolerance in the *dms3–1* line. In other words, our results emphasize that thermotolerance depends on a finely tuned hormonal network in which disruptions in one metabolic pathway can offset the benefits of another. This underscores the importance of a coordinated hormonal response for effective thermotolerance. Furthermore, greater similarity in the hormonal profiles between the *dms3-1* and *oeDMS3* lines compared to the wild type suggests that hormone balance requires tightly regulated RdDM activity. These results suggest a dose-dependent role of DMS3, as both non-functional and excessive protein levels disrupt key hormonal pathways and impair homeostasis. A recent study by Xun et al. (2025) has shown that a *Glycine max* mutant with disrupted DRMs, *i.e.*, DNA methyltransferases responsible for the initiation of *de novo* cytosine methylation and recruited by the DDR complex (in which DMS3 is a core component), exhibits a distinctly altered hormonal profile compared to wild-type plants. Moreover, the *Gmdrm* mutant shows increased levels of cytokinins – particularly the cZ and tZ types – and reduced levels of JA and JA-Ile, reflecting the hormonal changes observed in our *DMS3*-altered plants.

4.3. Primary photochemistry in dms3-1 takes longer to recover from heat stress

Several studies suggest that a reduced rate of photosynthesis during early development often leads to slower growth rates at later stages (Chen et al., 2005; Gao et al., 2020; Khanna et al., 2021). During the phenotyping experiment, F_V/F_M was the only photosynthetic parameter measured, and the treated *dms3-1* line showed lower values than the wild type (Suppl. Fig. 4). To overcome the limitations of the phenotyping platform, an *in vitro* experiment and a JIP-test were performed for a detailed evaluation of the photosynthetic processes. Interestingly, the seedlings grown *in vitro* showed a more pronounced F_V/F_M reduction than the seedlings grown in soil, even though they were exposed to a lower temperature (37 °C *vs.* 40 °C). These results can be attributed to the different growing conditions: the soil-grown seedlings were exposed to controlled humidity (60 %), while the *in vitro*-grown seedlings experienced higher humidity, which probably reduced transpiration during heat exposure and increased the effects of heat stress. A study on different tomato (*Solanum lycopersicum*) cultivars exposed to heat stress supports this hypothesis. It showed better production of plants growing at lower humidity than those growing at higher humidity, where evaporative cooling is limited (Ayenan et al., 2022).

Both *DMS3*-altered lines showed a greater reduction in F_V/F_M than the wild type, but only the *dms3-1* line showed significantly lower PI_{ABS}, a reliable indicator of stress (Chen and Cheng, 2009; Jägerbrand and Kudo, 2016; Zushi et al., 2012). This indicates a higher photosynthetic sensitivity in *dms3-1*. It is consistent with a study of heat stress effect on wild barley (*Hordeum spontaneum*) that showed significantly lower F_V/F_M and PI_{ABS} in heat-sensitive varieties than in heat-tolerant ones (Jedmowski and Brüggemann, 2015). Interestingly, the initial decrease in F_V/F_M was more pronounced in heat-treated *oeDMS3* seedlings than in the wild type, although photosynthetic efficiency did not decrease as much as in the treated *dms3-1* seedlings. This observation confirms that overexpression of *DMS3* does not lead to increased thermotolerance and that DMS3 acts in a dose-dependent manner, whereby both non-functional and unbalanced protein levels can impair physiological stress responses.

To further investigate the effects of heat stress on photosynthetic efficiency, we analyzed major energy fluxes that define PI_{ABS}: absorption (ABS/RC), trapping (TR_0/RC), electron transport (ET_0/RC), and energy dissipation (DI_0/RC). According to Strasser et al. (2000), plants exposed to elevated temperatures have increased ABS/RC and DI_0/RC, which can be attributed to a reduction in the density of active centers (RC/CS_0). Indeed, increased ABS/RC and DI_0/RC with a significant reduction of RC/CS_0 were only noticed in the *dms3-1* line. After recovery, no significant differences in photosynthetic responses were observed in *oeDMS3* seedlings, which is consistent with the notion that exposure to 37 °C represents moderate stress for *A. thaliana*, causing transient

physiological changes without long-term structural damage. However, heat-treated *dms3-1* seedlings retained reduced photosynthetic efficiency, even after recovery, suggesting a greater sensitivity of its photosynthetic apparatus to heat stress. This aligns with a study on common bean (*Phaseolus vulgaris*), where sensitive cultivars failed to restore photosynthetic rates after stress (Stefanov et al., 2011). Despite a more sensitive photosynthetic apparatus, the *dms3-1* line showed milder morphological changes after heat stress than the *oeDMS3* line. A possible explanation is increased phenotypic plasticity due to reduced DNA methylation, which alters the expression of genes and transposable elements and influence the plant's response to heat stress (Negi et al., 2016). According to the authors, these changes can lead to physiological adaptations that are not immediately recognizable at the morphological level. Physiological plasticity is particularly pronounced under stress, as physiological changes are often reversible and require fewer energy resources than morphological adaptations (Grime and Mackey, 2002).

Although heat stress caused less morphological change in the *dms3-1* line than in the *oeDMS3* line, under control conditions the *dms3-1* plants had smaller rosette area and biomass (Suppl. Fig. 3) compared to *oeDMS3* and the wild type. Finnegan et al. (1996) reported similar findings, showing that *A. thaliana* plants with reduced DNA methylation exhibit smaller leaves and rosettes. Ci et al. (2016) revealed that methylation variations in *Populus simonii* affect leaf size and photosynthetic efficiency. Here, the *dms3-1* line had lower basal RuBisCO levels, potentially limiting CO_2 fixation and sugar production, ultimately impairing growth (Sharma et al., 2020). Therefore, it is plausible that the reduced methylation in the *dms3-1* line (Kanno et al., 2008) contributed to a lower photosynthetic activity and growth rate compared to the *oeDMS3* line and the wild type.

4.4. DMS3 mutation results in impaired HSP90 and HSP70 levels

Exposure to elevated temperatures primarily activates HSFs, followed by the induction of HSPs and increased expression of genes involved in the biosynthesis of antioxidants and compatible osmolytes (Andrási et al., 2021; Kotak et al., 2007; Mittler et al., 2012). We found a significant increase of HSP90 expression in all heat-treated seedlings, regardless of *DMS3* expression. This result is in line with numerous previous studies that have shown a stronger induction of molecular chaperones during heat stress compared to other proteins (Finka et al., 2011; Finka et al., 2015; Guihur et al., 2021). HSP90 levels remained elevated even after recovery, which can be compared with the results of Charng et al. (2006), who showed that HSP90 levels peak approximately 3 h after exposure of *A. thaliana* seedlings to 37 °C and then gradually decline to control levels over the course of 72 h. This suggests that despite the relatively mild and short-term heat stress applied in our study, the cellular proteome may show a long-lasting effect such as elevated HSP90 levels that can support the refolding or stabilization of proteins damaged during the stress event (Hasanuzzaman et al., 2013). HSP70 proteins are constitutively expressed and characterized by a rapid upregulation during the early stages of heat stress, followed by a sudden decline during the recovery phase, therefore they can be considered "hit-and-run" chaperones (Kozeko, 2021; Lämke et al., 2016). This pattern was observed in wild-type seedlings, where HSP70 levels were slightly increased immediately after heat exposure but returned to baseline levels after 24 h. Curiously, in treated *oeDMS3* and *dms3-1* seedlings HSP70 levels increased after recovery. These results suggest that the RdDM, which is disrupted in *DMS3*-altered lines, may play a role in regulating HSP70 expression. Korotko et al. (2021) reported that three *HSP70* genes – *HSP70* (AT3G12580), *HSP70-1* (AT5G02500) and *HSP70-6* (AT4G24280) – undergo changes in methylation in the CG, CHG and CHH context during early heat stress in *A. thaliana*. Moreover, they showed that methylation increases as early as 6 h after exposure to 42 °C and reverses during the recovery phase. Heat stress also induces histone modifications (*e.g.*, H3K9ac, H3K4me3) that promote *HSP70* transcription early in the stress response but decrease during the recovery phase (Lämke et al., 2016), suggesting an important role of epigenetic regulation in the transient activation of HSP70. The antibody used in our study was reactive against HSP70 (AT3G12580) and HSP70-5 (AT1G16030), supporting the hypothesis that delayed HSP70 induction in *DMS3*-altered lines may be due to impaired epigenetic regulation.

As shown previously, HSP90 expression was notably upregulated in all three lines after heat stress. However, the *dms3-1* line had lower basal levels of HSP90 and HSP70 than the wild type, suggesting that RdDM may contribute to the maintenance of their basal expression. Le et al. (2014) reported that under optimal conditions, approximately 60 % of differentially expressed genes are downregulated in *nrpd1* and *nrpe1* mutants, which are deficient in Pol IV and Pol V, respectively, compared to wild type. However, further studies are needed to clarify the epigenetic mechanisms that control *HSP90* and *HSP70* expression and to determine whether some of these genes or their regulators are targets of RdDM. This is particularly interesting because the study by Kozeko (2021) showed that *A. thaliana* seedlings with mutated *HSP90-1* or *HSP70-5* show near-complete mortality after short-term exposure to 45 °C, while wild-type seedlings tolerate it well. This suggests that lower initial levels of HSP90 and HSP70 reduce thermotolerance. Although *dms3-1* seedlings exhibited the highest HSP90 induction immediately after treatment and the highest HSP70 induction after recovery, the lower basal expression of both proteins may have impaired the ability of *dms3-1* to show a rapid stress response, resulting in reduced survival at 45 °C.

4.5. Antioxidant system is partially activated in dms3-1 line

When exposed to elevated temperatures, plant cells often experience oxidative stress due to excessive ROS production, disrupting redox balance (Qu et al., 2013; Wani and Kumar, 2020). To counteract excessive ROS accumulation, plants activate antioxidant network (Mittler, 2002; Zhou et al., 2019). In heat-treated wild type, we noticed increased activity of key ROS-scavenging enzymes – G-POD, APX, SOD and CAT. The *oeDMS3* line showed higher activity of G-POD, APX, and SOD, while the *dms3-1* line only showed increased CAT activity. Similar to findings by Chan et al. (2016), who reported decreased antioxidant activity in *A. thaliana* mutants with altered RdDM mechanism after exposure to low temperatures, our results indicate reduced antioxidant activity in the *dms3-1* line after heat stress. Rizhsky et al. (2002) found that tobacco plants with impaired APX and/or CAT activity are more sensitive to abiotic stress and exhibit a greater reduction in photosynthetic rate than wild type, which aligns with our observations of *dms3-1*.

In addition to increased activity of the antioxidant system, proline plays a crucial role in stress responses, including osmoregulation, neutralization of free radicals, protein stabilization, and the maintenance of redox balance and cellular pH value (Gill et al., 2013; Li et al., 2018; Ozden et al., 2009). Surprisingly, in this study, all heat-treated seedlings showed reduced proline content immediately after exposure to elevated temperature, similar to findings in cotton (*Gossypium hirsutum*) and wheat (*Triticum aestivum*) (Gür et al., 2010; Kumar et al., 2012). This decline may be due to its role in cellular energy supply, as proline catabolism generates $FADH_2$ and NADH, promoting ATP production (Ingrisano et al., 2023; Launay et al., 2019). Since stress conditions lead to a decline in the efficiency of the primary photosynthetic reactions that generate ATP and NADPH, as our study has shown, amino acids such as proline can serve as temporary energy sources to compensate for the increased cellular energy demand during stress. After recovery, proline content in the *oeDMS3* line and the wild type returned to control levels, suggesting restored cellular balance. However, in the *dms3-1* seedlings, proline content increased after the recovery period, potentially serving as a defense mechanism against heat-induced damage. This aligns with previous studies showing elevated proline protects the photosynthetic apparatus under heat stress (Rajametov et al., 2021; Sehar et al., 2023; Tonhati et al., 2020). In our study, only the *dms3-1* line exhibited

reduced photosynthetic efficiency (PI_{ABS}) immediately after stress and after recovery, further supporting this hypothesis.

5. Conclusion

In this study, we investigated the role of DMS3 in thermotolerance of *Arabidopsis thaliana* and its influence on morphological, physiological, biochemical, and molecular responses to heat stress. Our results showed that heat stress significantly affected the stability and localization of the DMS3 protein in root tissue, suggesting its regulatory role at elevated temperatures. Plants with altered *DMS3* expression (*oeDMS3* and *dms3-1*) showed a greater reduction in morphological traits after heat stress than wild-type plants. In addition, *dms3-1* and *oeDMS3* plants had lower levels of JA and its bioactive form, JA-Ile, compared to the wild type, indicating perturbations in jasmonate metabolism under stress and control conditions. Furthermore, in response to heat stress, the *dms3-1* line showed increased cytokinin content, mainly in the form of ribosides, and accumulated inactive auxin metabolites. Although *dms3-1* and *oeDMS3* lines had some similarities in the physiological and biochemical responses to heat stress, indicating that both non-functional and excessive levels of DMS3 affect thermotolerance, the *dms3-1* mutant showed the highest thermosensitivity after heat shock. *In vitro* analyzes showed that the *dms3-1* exhibited delayed recovery of primary photochemistry and only partial activation of the antioxidant defense system. Remarkably, the *dms3-1* line was the only one that showed increased proline levels after recovery. Under control conditions, *dms3-1* showed reduced growth and lower baseline levels of RuBisCO, HSP90 and HSP70 compared to *oeDMS3* and wild-type plants. Overall, our study highlighted the important role of a functional and balanced DMS3 protein in maintaining thermotolerance and effectively coordinating the plant's morphological, physiological, biochemical and molecular responses to heat stress. Furthermore, our results confirmed the necessity of a functional DMS3 protein for supporting plant growth and development under control conditions.

Funding sources

This work was supported by the Croatian Science Foundation (project PHYTOMETHDEV; IP 2016-06–6229 to DL-L), the short-term mobility grant by the Federation of European Societies of Plant Biology (FESPB) to SV, the Czech Science Foundation (23-07376S to ON), and the research grant of the University of Zagreb. Financial support by the Access to Research Infrastructures activity in the Horizon 2020 Programme of the EU (EPPN2020 Grant Agreement 731013) to ŽV-C is gratefully acknowledged.

CRediT authorship contribution statement

Sandra Vitko: Writing – original draft, Visualization, Software, Methodology, Investigation, Funding acquisition, Formal analysis, Conceptualization. **Mirta Tokić:** Writing – review & editing, Visualization, Methodology, Investigation, Formal analysis. **Silvia Braun:** Writing – review & editing, Methodology, Investigation. **Thorsten Brehm:** Writing – review & editing, Methodology, Investigation. **Iva Pavlović:** Writing – review & editing, Methodology, Investigation. **Fabio Fiorani:** Writing – review & editing, Supervision, Project administration, Funding acquisition. **Ondřej Novák:** Writing – review & editing, Supervision, Funding acquisition. **Nataša Bauer:** Writing – review & editing, Supervision, Conceptualization. **Dunja Leljak-Levanić:** Writing – review & editing, Project administration, Funding acquisition. **Željka Vidaković-Cifrek:** Writing – review & editing, Supervision, Project administration, Funding acquisition, Conceptualization.

Declaration of competing interest

The authors declare that they have no known competing financial interests or personal relationships that could have appeared to influence the work reported in this paper.

Acknowledgements

We would like to thank Zdravko Lorković for the *A. thaliana dms3-1* mutant.

Supplementary materials

Supplementary material associated with this article can be found, in the online version, at doi:10.1016/j.stress.2025.101013.

Data availability

Data supporting the results of this study are available upon request.

References

Aebi, H., 1984. [13] Catalase *in vitro*. Methods Enzymol. 105, 121–126. https://doi.org/10.1016/S0076-6879(84)05016-3.

Andrási, N., Pettkó-Szandtner, A., Szabados, L., 2021. Diversity of plant heat shock factors: regulation, interactions, and functions. J. Exp. Bot. 72, 1558–1575. https://doi.org/10.1093/jxb/eraa576.

Ayenan, M.A.T., Danquah, A., Hanson, P., Asante, I.K., Danquah, E.Y., 2022. Tomato (*Solanum lycopersicum* L.) genotypes respond differently to long-term dry and humid heat stress. Horticulturae 8, 118. https://doi.org/10.3390/horticulturae8020118.

Barboza-Barquero, L., Nagel, K.A., Jansen, M., Klasen, J.R., Kastenholz, B., Braun, S., Bleise, B., Brehm, T., Koornneef, M., Fiorani, F., 2015. Phenotype of *Arabidopsis thaliana* semi-dwarfs with deep roots and high growth rates under water-limiting conditions is independent of the GA5 loss-of-function alleles. Ann. Bot. 116, 321–331. https://doi.org/10.1093/aob/mcv099.

Bates, L.S., Waldren, R.A., Teare, I.D., 1973. Rapid determination of free proline for water-stress studies. Plant Soil 39, 205–207. https://doi.org/10.1007/BF00018060.

Beauchamp, C., Fridovich, I., 1971. Superoxide dismutase: improved assays and an assay applicable to acrylamide gels. Anal. Biochem. 44, 276–287. https://doi.org/10.1016/0003-2697(71)90370-8.

Boyes, D.C., Zayed, A.M., Ascenzi, R., McCaskill, A.J., Hoffman, N.E., Davis, K.R., Görlach, J., 2001. Growth stage-based phenotypic analysis of Arabidopsis: a model for high throughput functional genomics in plants. Plant Cell 113, 1499–1510. https://doi.org/10.1105/TPC.010011.

Bradford, M.M., 1976. A rapid and sensitive method for the quantitation of microgram quantities of protein utilizing the principle of protein-dye binding. Anal. Biochem. 72, 248–254. https://doi.org/10.1006/abio.1976.9999.

Chan, Z., Wang, Y., Cao, M., Gong, Y., Mu, Z., Wang, H., Hu, Y., Deng, X., He, X.J., Zhu, J. K., 2016. *RDM4* modulates cold stress resistance in *Arabidopsis* partially through the *CBF*-mediated pathway. New Phytol. 209, 1527–1539. https://doi.org/10.1111/nph.13727.

Charng, Y.Y., Liu, H.C., Liu, N.Y., Hsu, F.C., Ko, S.S., 2006. Arabidopsis Hsa32, a novel heat shock protein, is essential for acquired thermotolerance during long recovery after acclimation. Plant Physiol. 140, 1297–1305. https://doi.org/10.1104/pp.105.074898.

Chen, L.S., Cheng, L., 2009. Photosystem 2 is more tolerant to high temperature in apple (*Malus domestica* Borkh.) leaves than in fruit peel. Photosynthetica 47, 112–120. https://doi.org/10.1007/s11099-009-0017-4.

Chen, S., Hajirezaei, M., Peisker, M., Tschiersch, H., Sonnewald, U., Börnke, F., 2005. Decreased sucrose-6-phosphate phosphatase level in transgenic tobacco inhibits photosynthesis, alters carbohydrate partitioning, and reduces growth. Planta 221, 479–492. https://doi.org/10.1007/s00425-004-1458-4.

Ci, D., Song, Y., Du, Q., Tian, M., Han, S., Zhang, D., 2016. Variation in genomic methylation in natural populations of *Populus simonii* is associated with leaf shape and photosynthetic traits. J. Exp. Bot. 67, 723–737. https://doi.org/10.1093/jxb/erv485.

Dobrá, J., Černý, M., Štorchová, H., Dobrev, P., Skalák, J., Jedelský, P.L., Lukšanová, H., Gaudinová, A., Pešek, B., Malbeck, J., Vanek, T., Brzobohatý, B., Vanková, R., 2015. The impact of heat stress targeting on the hormonal and transcriptomic response in Arabidopsis. Plant Sci. 231, 52–61. https://doi.org/10.1016/j.plantsci.2014.11.005.

Dubin, M.J., Mittelsten Scheid, O., Becker, C., 2018. Transposons: a blessing curse. Curr. Opin. Plant. Biol. 42, 23–29. https://doi.org/10.1016/j.pbi.2018.01.003.

Elewa, T.A., Sadak, M.S., Saad, A.M., 2017. Proline treatment improves physiological responses in quinoa plants under drought stress. Biosci. Res. 14, 21–33.

Erdmann, R.M., Picard, C.L., 2020. RNA-directed DNA methylation. PLoS Genet. 16, e1009034. https://doi.org/10.1371/journal.pgen.1009034.

Fahad, S., Bajwa, A.A., Nazir, U., Anjum, S.A., Farooq, A., Zohaib, A., Sadia, S., Nasim, W., Adkins, S., Saud, S., Ihsan, M.Z., Alharby, H., Wu, C., Wang, D., Huang, J., 2017. Crop production under drought and heat stress: plant responses and management options. Front. Plant. Sci. 8, 1147. https://doi.org/10.3389/fpls.2017.01147.

Finka, A., Mattoo, R.U.H., Goloubinoff, P., 2011. Meta-analysis of heat- and chemically upregulated chaperone genes in plant and human cells. Cell Stress Chaperones 16, 15–31. https://doi.org/10.1007/s12192-010-0216-8.

Finka, A., Sharma, S.K., Goloubinoff, P., 2015. Multi-layered molecular mechanisms of polypeptide holding, unfolding and disaggregation by HSP70/HSP110 chaperones. Front. Mol. Biosci. 2, 29. https://doi.org/10.3389/fmolb.2015.00029.

Finnegan, E.J., Peacock, W.J., Dennis, E.S., 1996. Reduced DNA methylation in *Arabidopsis thaliana* results in abnormal plant development. Dev. Biol. 93, 8449–8454. https://doi.org/10.1073/pnas.93.16.8449.

Gao, G., Tester, M.A., Julkowska, M.M., 2020. The use of high-throughput phenotyping for assessment of heat stress-induced changes in Arabidopsis. Plant Phenom. 2020, 3723916. https://doi.org/10.34133/2020/3723916.

Gill, S.S., Tajrishi, M., Madan, M., Tuteja, N., 2013. A DESD-box helicase functions in salinity stress tolerance by improving photosynthesis and antioxidant machinery in rice (*Oryza sativa* L. cv. PB1). Plant Mol. Biol. 82, 1–22. https://doi.org/10.1007/s11103-013-0031-6.

Grgić, M., Vitko, S., Drmić, J., Leljak-Levanić, D., 2025. Connecting the dots: epigenetics, ABA, and plant stress tolerance. Acta Bot. Croat. 84, 1–29. https://doi.org/10.37427/botcro-2025-004.

Grime, J.P., Mackey, J.M.L., 2002. The role of plasticity in resource capture by plants. Evol. Ecol. 16, 299–307. https://doi.org/10.1023/A:1019640813676.

Gu, X., Xu, T., He, Y., 2014. A histone H3 lysine-27 methyltransferase complex represses lateral root formation in *Arabidopsis thaliana*. Mol. Plant. 7, 977–988. https://doi.org/10.1093/mp/ssu035.

Gu, Z., Eils, R., Schlesner, M., 2016. Complex heatmaps reveal patterns and correlations in multidimensional genomic data. Bioinformatics 32, 2847–2849. https://doi.org/10.1093/bioinformatics/btw313.

Guihur, A., Fauvet, B., Finka, A., Quadroni, M., Goloubinoff, P., 2021. Quantitative proteomic analysis to capture the role of heat-accumulated proteins in moss plant acquired thermotolerance. Plant Cell Environ.. 44, 2117–2133. https://doi.org/10.1111/pce.13975.

Gür, A., Demirel, U., Özden, M., Kahraman, A., Çopur, O., 2010. Diurnal gradual heat stress affects antioxidant enzymes, proline accumulation and some physiological components in cotton (*Gossypium hirsutum* L.). Afr. J. Biotechnol. 9, 1008–1015. https://doi.org/10.5897/AJB09.1590.

Hasanuzzaman, M., Nahar, K., Alam, M.M., Roychowdhury, R., Fujita, M., 2013. Physiological, biochemical, and molecular mechanisms of heat stress tolerance in plants. Int. J. Mol. Sci. 14, 9643–9684. https://doi.org/10.3390/ijms14059643.

Hazman, M., Hause, B., Eiche, E., Nick, P., Riemann, M., 2015. Increased tolerance to salt stress in OPDA-deficient rice *ALLENE OXIDE CYCLASE* mutants is linked to an increased ROS-scavenging activity. J. Exp. Bot. 66, 3339–3352. https://doi.org/10.1093/jxb/erv142.

Hossain, M.S., Kawakatsu, T., Kim, K.D., Zhang, N., Nguyen, C.T., Khan, S.M., Batek, J. M., Joshi, T., Schmutz, J., Grimwood, J., Schmitz, R.J., Xu, D., Jackson, S.A., Ecker, J.R., Stacey, G., 2017. Divergent cytosine DNA methylation patterns in single-cell, soybean root hairs. New Phytol. 214, 808–819. https://doi.org/10.1111/nph.14421.

Ingrisano, R., Tosato, E., Trost, P., Gurrieri, L., Sparla, F., 2023. Proline, cysteine and branched-chain amino acids in abiotic stress response of land plants and microalgae. Plants 12, 3410. https://doi.org/10.3390/plants12193410.

Ito, H., Gaubert, H., Bucher, E., Mirouze, M., Vaillant, I., Paszkowski, J., 2011. An siRNA pathway prevents transgenerational retrotransposition in plants subjected to stress. Nature 472, 115–120. https://doi.org/10.1038/nature09861.

Jägerbrand, A.K., Kudo, G., 2016. Short-term responses in maximum quantum yield of PSII (F_v/F_m) to *ex situ* temperature treatment of populations of bryophytes originating from different sites in Hokkaido. Northern Japan. Plants 5, 22. https://doi.org/10.3390/plants5020022.

Jagić, M., Vuk, T., Škiljaica, A., Markulin, L., Vičić Bočkor, V., Tokić, M., Miškec, K., Razdorov, G., Habazin, S., Šoštar, M., Weber, I., Bauer, N., Leljak Levanić, D., 2022. BPM1 regulates RdDM-mediated DNA methylation via a cullin 3 independent mechanism. Plant Cell Rep. 41, 2139–2157. https://doi.org/10.1007/s00299-022-02911-9.

Jansen, M., Gilmer, F., Biskup, B., Nagel, K.A., Rascher, U., Fischbach, A., Briem, S., Dreissen, G., Tittmann, S., Braun, S., De Jaeger, I., Metzlaff, M., Schurr, U., Scharr, H., Walter, A., 2009. Simultaneous phenotyping of leaf growth and chlorophyll fluorescence via GROWSCREEN FLUORO allows detection of stress tolerance in *Arabidopsis thaliana* and other rosette plants. Funct. Plant Biol. 36, 902–914. https://doi.org/10.1071/FP09095.

Jedmowski, C., Brüggemann, W., 2015. Imaging of fast chlorophyll fluorescence induction curve (OJIP) parameters, applied in a screening study with wild barley (*Hordeum spontaneum*) genotypes under heat stress. J. Photochem. Photobiol. B 151, 153–160. https://doi.org/10.1016/j.jphotobiol.2015.07.020.

Jha, U.C., Nayyar, H., Siddique, K.H.M., 2022. Role of phytohormones in regulating heat stress acclimation in agricultural crops. J. Plant Growth Regul. 41, 1041–1064. https://doi.org/10.1007/s00344-021-10362-x.

Kanno, T., Bucher, E., Daxinger, L., Huettel, B., Böhmdorfer, G., Gregor, W., Kreil, D.P., Matzke, M., Matzke, A.J.M., 2008. A structural-maintenance-of-chromosomes hinge domain-containing protein is required for RNA-directed DNA methylation. Nat. Genet. 40, 670–675. https://doi.org/10.1038/ng.119.

Khanna, R.R., Jahan, B., Iqbal, N., Khan, N.A., AlAjmi, M.F., Tabish Rehman, M., Khan, M.I.R., 2021. GABA reverses salt-inhibited photosynthetic and growth responses through its influence on NO-mediated nitrogen-sulfur assimilation and antioxidant system in wheat. J. Biotech. 325, 73–82. https://doi.org/10.1016/j.jbiotec.2020.11.015.

Korotko, U., Chwiałkowska, K., Sańko-Sawczenko, I., Kwasniewski, M., 2021. DNA demethylation in response to heat stress in *Arabidopsis thaliana*. Int. J. Mol. Sci. 22, 1–20. https://doi.org/10.3390/ijms22041555.

Kotak, S., Larkindale, J., Lee, U., von Koskull-Döring, P., Vierling, E., Scharf, K.D., 2007. Complexity of the heat stress response in plants. Curr. Opin. Plant Biol. 10, 310–316. https://doi.org/10.1016/j.pbi.2007.04.011.

Kozeko, L., 2021. Different roles of inducible and constitutive HSP70 and HSP90 in tolerance of *Arabidopsis thaliana* to high temperature and water deficit. Acta Physiol. Plant. 43, 58. https://doi.org/10.1007/s11738-021-03229-x.

Kumar, R.R., Goswami, S., Sharma, S.K., Singh, K., Gadpayle, K.A., Kumar, N., Rai, G.K., Singh, M., Rai, R.D., 2012. Protection against heat stress in wheat involves change in cell membrane stability, antioxidant enzymes, osmolyte, H_2O_2 and transcript of heat shock protein. Int. J. Plant Physiol. Biochem. 4, 83–91. https://doi.org/10.5897/ijppb12.008.

Kumar, S., Mohapatra, T., 2021. Dynamics of DNA methylation and its functions in plant growth and development. Front. Plant Sci. 12, 596236. https://doi.org/10.3389/fpls.2021.596236.

Laemmli, U.K., 1970. Cleavage of structural proteins during the assembly of the head of bacteriophage T4. Nature 227, 680–685. https://doi.org/10.1038/227680a0.

Lämke, J., Brzezinka, K., Altmann, S., Bäurle, I., 2016. A hit-and-run heat shock factor governs sustained histone methylation and transcriptional stress memory. EMBO J. 35, 162–175. https://doi.org/10.15252/embj.201592593.

Launay, A., Cabassa-Hourton, C., Eubel, H., Maldiney, R., Guivarc'h, A., Crilat, E., Planchais, S., Lacoste, J., Bordenave-Jacquemin, M., Clément, G., Ruchard, L., Carol, P., Barun, H.P., Lebreton, S., Savouré, A., 2019. Proline oxidation fuels mitochondrial respiration during dark-induced leaf senescence in *Arabidopsis thaliana*. J. Exp. Bot. 70, 6203–6214. https://doi.org/10.1093/jxb/erz351.

Le, T.N., Schumann, U., Smith, N.A., Tiwari, S., Au, P.C.K., Zhu, Q.H., Taylor, J.M., Kazan, K., Llewellyn, D.J., Zhang, R., Dennis, E.S., Wang, M.B., 2014. DNA demethylases target promoter transposable elements to positively regulate stress responsive genes in *Arabidopsis*. Genome Biol. 15, 1–18. https://doi.org/10.1186/s13059-014-0458-3.

Li, G., Zhang, C., Zhang, G., Fu, W., Feng, B., Chen, T., Peng, S., Tao, L., Fu, G., 2020. Abscisic acid negatively modulates heat tolerance in rolled leaf rice by increasing leaf temperature and regulating energy homeostasis. Rice 13, 1–16. https://doi.org/10.1186/s12284-020-00379-3.

Li, J., Guo, X., Zhang, M., Wang, X., Zhao, Y., Yin, Z., Zhang, Z., Wang, Y., Xiong, H., Zhang, H., Todorovska, E., Li, Z., 2018. *OsERF71* confers drought tolerance via modulating ABA signaling and proline biosynthesis. Plant Sci. 270, 131–139. https://doi.org/10.1016/j.plantsci.2018.01.017.

Li, N., Euring, D., Cha, J.Y., Lin, Z., Lu, M., Huang, L.J., Kim, W.Y., 2021. Plant hormone-mediated regulation of heat tolerance in response to global climate change. Front. Plant Sci. 11, 1–11. https://doi.org/10.3389/fpls.2020.627969.

Maehly, A.C., Chance, B., 1954. The assay of catalases and peroxidases. Methods Biochem. Anal. 1, 357–424. https://doi.org/10.1002/9780470110171.ch14.

Mathur, S., Agrawal, D., Jajoo, A., 2014. Photosynthesis: response to high temperature stress. J. Photochem. Photobiol. B 137, 116–126. https://doi.org/10.1016/j.jphotobiol.2014.01.010.

Matityahu, A., Onn, I., 2018. A new twist in the coil: functions of the coiled-coil domain of structural maintenance of chromosome (SMC) proteins. Curr. Genet. 64, 109–116. https://doi.org/10.1007/s00294-017-0735-2.

Matzke, M.A., Kanno, T., Matzke, A.J.M., 2015. RNA-directed DNA methylation: The evolution of a complex epigenetic pathway in flowering plants. Annu. Rev. Plant. Biol. 66, 243–267. https://doi.org/10.1146/annurev-arplant-043014-114633.

Mittler, R., 2002. Oxidative stress, antioxidants and stress tolerance. Trends Plant Sci. 7, 405–410. https://doi.org/10.1016/s1360-1385(02)02312-9.

Mittler, R., Blumwald, E., 2015. The roles of ROS and ABA in systemic acquired acclimation. Plant Cell 27, 64–70. https://doi.org/10.1105/tpc.114.133090.

Mittler, R., Finka, A., Goloubinoff, P., 2012. How do plants feel the heat? Trends Biochem. Sci. 37, 118–125. https://doi.org/10.1016/j.tibs.2011.11.007.

Møller, I.M., Jensen, P.E., Hansson, A., 2007. Oxidative modifications to cellular components in plants. Annu. Rev. Plant Biol. 58, 459–481. https://doi.org/10.1146/annurev.arplant.58.032806.103946.

Murashige, T., Skoog, F., 1962. A revised medium for rapid growth and bio assays with tobacco tissue cultures. Physiol. Plant. 15, 473–497. https://doi.org/10.1111/j.1399-3054.1962.tb08052.x.

Nakano, Y., Asada, K., 1981. Hydrogen peroxide is scavenged by ascorbate-specific peroxidase in spinach chloroplasts. Plant Cell Physiol. 22, 867–880. https://doi.org/10.1093/oxfordjournals.pcp.a076232.

Negi, P., Rai, A.N., Suprasanna, P., 2016. Moving through the stressed genome: emerging regulatory roles for transposons in plant stress response. Front. Plant Sci. 7, 1448. https://doi.org/10.3389/fpls.2016.01448.

Ohama, N., Sato, H., Shinozaki, K., Yamaguchi-Shinozaki, K., 2017. Transcriptional regulatory network of plant heat stress response. Trends Plant Sci. 22, 53–65. https://doi.org/10.1016/j.tplants.2016.08.015.

Ozden, M., Demirel, U., Kahraman, A., 2009. Effects of proline on antioxidant system in leaves of grapevine (*Vitis vinifera* L.) exposed to oxidative stress by H_2O_2. Sci. Hortic. 119, 163–168. https://doi.org/10.1016/j.scienta.2008.07.031.

Palomar, V.M., Garciarrubio, A., Garay-Arroyo, A., Martínez-Martínez, C., Rosas-Bringas, O., Reyes, J.L., Covarrubias, A.A., 2021. The canonical RdDM pathway mediates the control of seed germination timing under salinity. Plant J. 105, 691–707. https://doi.org/10.1111/tpj.15064.

Pavlů, J., Novák, J., Koukalová, V., Luklová, M., Brzobohatý, B., Černý, M., 2018. Cytokinin at the crossroads of abiotic stress signalling pathways. Int. J. Mol. Sci. 19, 2450. https://doi.org/10.3390/ijms19082450.

Peleg, Z., Blumwald, E., 2011. Hormone balance and abiotic stress tolerance in crop plants. Curr. Opin. Plant Biol. 14, 290–295. https://doi.org/10.1016/j.pbi.2011.02.001.

Pfaffl, M.W., 2001. A new mathematical model for relative quantification in real-time RT–PCR. Nucleic Acids Res. 29, e45. https://doi.org/10.1093/nar/29.9.e45.

Popova, O.V., Dinh, H.Q., Aufsatz, W., Jonak, C., 2013. The RdDM pathway is required for basal heat tolerance in *Arabidopsis*. Mol. Plant 6, 396–410. https://doi.org/10.1093/mp/sst023.

Prerostova, S., Dobrev, P.I., Gaudinova, A., Knirsch, V., Körber, N., Pieruschka, R., Fiorani, F., Brzobohatý, B., Cerný, M., Spichak, L., Humplik, J., Vanek, T., Schurr, U., Vankova, R., 2018. Cytokinins: Their impact on molecular and growth responses to drought stress and recovery in *Arabidopsis*. Front. Plant Sci. 9, 655. https://doi.org/10.3389/fpls.2018.00655.

Prerostova, S., Dobrev, P.I., Kramna, B., Gaudinova, A., Knirsch, V., Spichal, L., Zatloukal, M., Vankova, R., 2020. Heat acclimation and inhibition of cytokinin degradation positively affect heat stress tolerance of *Arabidopsis*. Front. Plant Sci. 11, 87. https://doi.org/10.3389/fpls.2020.00087.

Prerostova, S., Vankova, R., 2023. Phytohormone-mediated regulation of heat stress response in plants. In: Ahammed, G.J., Yu, J. (Eds.), Plant Hormones and Climate Change. Springer Nature Singapore, Singapore, pp. 167–206. https://doi.org/10.1007/978-981-19-4941-8_8.

Qirat, M., Shahbaz, M., Perveen, S., 2018. Beneficial role of foliar-applied proline on carrot (*Daucus carota* L.) under saline conditions. Pak. J. Bot. 50, 1735–1744.

Qu, A.L., Ding, Y.F., Jiang, Q., Zhu, C., 2013. Molecular mechanisms of the plant heat stress response. Biochem. Biophys. Res. Commun. 432, 203–207. https://doi.org/10.1016/j.bbrc.2013.01.104.

Rajametov, S.N., Yang, E.Y., Cho, M.C., Chae, S.Y., Jeong, H.B., Chae, W.B., 2021. Heat-tolerant hot pepper exhibits constant photosynthesis via increased transpiration rate, high proline content and fast recovery in heat stress condition. Sci. Rep. 11, 14328. https://doi.org/10.1038/s41598-021-93697-5.

Raza, A., Charagh, S., Abbas, S., Hassan, M.U., Saeed, F., Haider, S., Sharif, R., Anand, A., Corpas, F.J., Jin, W., Varshney, R.K., 2023. Assessment of proline function in higher plants under extreme temperatures. Plant Biol. 253, 79–395. https://doi.org/10.1111/plb.13510.

Rizhsky, L., Hallak-Herr, E., Van Breusegem, F., Rachmilevitch, S., Barr, J.E., Rodermel, S., Inzé, D., Mittler, R., 2002. Double antisense plants lacking ascorbate peroxidase and catalase are less sensitive to oxidative stress than single antisense plants lacking ascorbate peroxidase or catalase. Plant J 32, 329–342. https://doi.org/10.1046/j.1365-313X.2002.01427.x.

Rodríguez, M., Canales, E., Borrás-Hidalgo, O., 2005. Molecular aspects of abiotic stress in plants. Biotecnol. Apl. 22, 1–10.

Romanov, G.A., Schmülling, T., 2022. On the biological activity of cytokinin free bases and their ribosides. Planta 255, 27. https://doi.org/10.1007/s00425-021-03810-1.

Romero-Calvo, I., Ocón, B., Martínez-Moya, P., Suárez, M.D., Zarzuelo, A., Martínez-Augustin, O., de Medina, F.S., 2010. Reversible Ponceau staining as a loading control alternative to actin in Western blots. Anal. Biochem. 401, 318–320. https://doi.org/10.1016/j.ab.2010.02.036.

Rowley, M.J., Rothi, M.H., Böhmdorfer, G., Kuciński, J., Wierzbicki, A.T., 2017. Long-range control of gene expression via RNA-directed DNA methylation. PLoS Genet. 13, e1006749. https://doi.org/10.1371/journal.pgen.1006749.

Rymen, B., Ferrafiat, L., Blevins, T., 2020. Non-coding RNA polymerases that silence transposable elements and reprogram gene expression in plants. Transcription 11, 172–191. https://doi.org/10.1080/21541264.2020.1825906.

Sadeghipour, O., 2020. Cadmium toxicity alleviates by seed priming with proline or glycine betaine in cowpea (*Vigna unguiculata* (L.) Walp.). Egypt. J. Agron. 42, 163–170. https://doi.org/10.21608/agro.2020.23667.1204.

Sakata, T., Oshino, T., Miura, S., Tomabechi, M., Tsunaga, Y., Higashitani, N., Miyazawa, Y., Takahashi, H., Watanabe, M., Higashitani, A., 2010. Auxins reverse plant male sterility caused by high temperatures. PNAS 107, 8569–8574. https://doi.org/10.1073/pnas.1000869107.

Scharr, H., Bruns, B., Fischbach, A., Roussel, J., Scholtes, L., Stein, J.V., 2020. Germination detection of seedlings in soil: A system, dataset and challenge. In: Bartoli, A., Fusiello, A. (Eds.), Computer Vision – ECCV 2020 Workshops: Glasgow, UK, August 23–28, 2020, Proceedings, Part VI. Springer-Verlag, Berlin, Heidelberg, pp. 360–374. https://doi.org/10.1007/978-3-030-65414-6_25.

Schindelin, J., Arganda-Carreras, I., Frise, E., Kaynig, V., Longair, M., Pietzsch, T., Preibisch, S., Rueden, C., Saalfeld, S., Schmid, B., Tinevez, J-Y., White, D.J., Hartenstein, V., Eliceiri, K., Tomancak, P., Cardona, A., 2012. Fiji: an open-source platform for biological-image analysis. Nat. Methods 9, 676–682. https://doi.org/10.1038/nmeth.2019.Fiji.

Schneider, C.A., Rasband, W.S., Eliceiri, K.W., 2012. NIH Image to ImageJ: 25 years of image analysis HHS public access. Nat. Methods 9, 671–675. https://doi.org/10.1038/nmeth.2089.

Sehar, Z., Gautam, H., Masood, A., Khan, N.A., 2023. Ethylene- and proline-dependent regulation of antioxidant enzymes to mitigate heat stress and boost photosynthetic efficacy in wheat plants. J. Plant Growth Regul. 42, 2683–2697. https://doi.org/10.1007/s00344-022-10737-8.

Sharma, S., Joshi, J., Kataria, S., Verma, S.K., Chatterjee, S., Jain, M., Pathak, K., Rastogi, A., Brestic, M., 2020. Regulation of the Calvin cycle under abiotic stresses: an overview. In: Tripathi, D.K., Singh, V.P., Chauhan, D.K., Sharma, S., Prasad, S.M., Dubey, N.K., Ramawat, N. (Eds.), Plant Life under Changing Environment: Responses and Management. Elsevier Inc., pp. 681–717. https://doi.org/10.1016/B978-0-12-818204-8.00030-8

Siddiqui, M.H., Alamri, S.A., Al-Khaishany, M.Y., Al-Qutami, M.A., Ali, H.M., Khan, M. N., 2017. Sodium nitroprusside and indole acetic acid improve the tolerance of tomato plants to heat stress by protecting against DNA damage. J. Plant Interact. 12, 177–186. https://doi.org/10.1080/17429145.2017.1310941.

Skalák, J., Černý, M., Jedelský, P., Dobrá, J., Ge, E., Novák, J., Brzobohatý, B., 2016. Stimulation of *ipt* overexpression as a tool to elucidate the role of cytokinins in high temperature responses of *Arabidopsis thaliana*. J. Exp. Bot. 67, 2861–2873. https://doi.org/10.1093/jxb/erw129.

Song, Z., Fan, N., Jiao, G., Liu, M., Wang, X., Jia, H., 2019. Overexpression of OsPT8 increases auxin content and enhances tolerance to high-temperature stress in *Nicotiana tabacum*. Genes 10, 809. https://doi.org/10.3390/genes10100809.

Staples, R.C., Stahmann, M.A., 1964. Changes in proteins and several enzymes in susceptible bean leaves after infection by the bean rust fungus. Phytopathology 54, 760–764.

Stefanov, D., Petkova, V., Denev, I.D., 2011. Screening for heat tolerance in common bean (*Phaseolus vulgaris* L.) lines and cultivars using *JIP*-test. Sci. Hortic. 128, 1–6. https://doi.org/10.1016/j.scienta.2010.12.003.

Strasser, R.J., Srivastava, A., Tsimilli-Michael, M., 2000. The fluorescence transient as a tool to characterize and screen photosynthetic samples. In: Yunus, M., Pathre, U., Mohanty, P. (Eds.), Probing Photosynthesis: Mechanisms, Regulation and Adaptation. Taylor and Francis Group, pp. 445–483.

Šimura, J., Antoniadi, I., Široká, J., Tarkowská, D.E., Strnad, M., Ljung, K., Novák, O., 2018. Plant hormonomics: multiple phytohormone profiling by targeted metabolomics. Plant Physiol. 177, 476–489. https://doi.org/10.1104/pp.18.00293.

Škiljaica, A., Jagić, M., Vuk, T., Leljak Levanić, D., Bauer, N., Markulin, L., 2022. Evaluation of reference genes for RT-qPCR gene expression analysis in *Arabidopsis thaliana* exposed to elevated temperatures. Plant Biol. 24, 367–379. https://doi.org/10.1111/plb.13382.

Škiljaica, A., Lechner, E., Jagić, M., Majsec, K., Malenica, N., Genschik, P., Bauer, N., 2020. The protein turnover of Arabidopsis BPM1 is involved in regulation of flowering time and abiotic stress response. Plant Mol. Biol. 102, 359–372. https://doi.org/10.1007/s11103-019-00947-2.

Taylor, S.C., Posch, A., 2014. The design of a quantitative western blot experiment. Biomed. Res. Int. 2014, 361590. https://doi.org/10.1155/2014/361590.

Tognetti, V.B., Mühlenbock, P.E., Van Breusegem, F., 2012. Stress homeostasis–the redox and auxin perspective. Plant Cell Environ. 35, 321–333. https://doi.org/10.1111/j.1365-3040.2011.02324.x.

Tonhati, R., Mello, S.C., Momesso, P., Pedroso, R.M., 2020. L-proline alleviates heat stress of tomato plants grown under protected environment. Sci. Hortic. 268, 109370. https://doi.org/10.1016/j.scienta.2020.109370.

Vandesompele, J., De Preter, K., Pattyn, F., Poppe, B., Van Roy, N., De Paepe, A., Speleman, F., 2002. Accurate normalization of real-time quantitative RT-PCR data by geometric averaging of multiple internal control genes. Genome Biol. 3, 1–12. https://doi.org/10.1186/gb-2002-3-7-research0034.

Veselov, D.S., Kudoyarova, G.R., Kudryakova, N.V., Kusnetsov, V.V., 2017. Role of cytokinins in stress resistance of plants. Russ. J. Plant Physiol. 64, 15–27. https://doi.org/10.1134/S1021443717010162.

Vuković, M., Kutnjak, M., Vitko, S., Tkalec, M., Vidaković-Cifrek, Ž., 2025. Heat priming modifies heat stress response in *BPM1*-overexpressing *Arabidopsis thaliana* (L.) Heynh. J. Plant Growth Regul. 44, 1695–1712. https://doi.org/10.1007/s00344-024-11337-4.

Wang, M., Fan, X., Ding, F., 2023. Jasmonate: a hormone of primary importance for temperature stress response in plants. Plants 12, 4080. https://doi.org/10.3390/plants12244080.

Wani, S.H., Kumar, V., 2020. Heat Stress Tolerance in Plants: physiological, Molecular and Genetic Perspectives. John Wiley & Sons Ltd, Hoboken, New Jersey. https://doi.org/10.1002/9781119432401.

Wongpalee, S.P., Liu, S., Gallego-Bartolomé, J., Leitner, A., Aebersold, R., Liu, W., Yen, L., Nohales, M.A., Hsuanyu Kuo, P., Vashisht, A.A., Wohlschlegel, J.A., Feng, S., Kay, S.A., Hong Zhou, Z., Jacobsen, S.E., 2019. CryoEM structures of Arabidopsis DDR complexes involved in RNA-directed DNA methylation. Nat. Commun. 10, 3916. https://doi.org/10.1038/s41467-019-11759-9.

Xu, Y.H., Liao, Y.C., Zhang, Z., Liu, J., Sun, P.W., Gao, Z.H., Sui, C., Wei, J.H., 2016. Jasmonic acid is a crucial signal transducer in heat shock induced sesquiterpene formation in *Aquilaria sinensis*. Sci. Rep. 6, 21843. https://doi.org/10.1038/srep21843.

Xun, H., Lian, L., Yuan, J., Hong, J., Hao, S., Zhao, H., Liu, S., Feng, W., Yin, H., Liu, B., Wang, X., 2025. Domains rearranged methyltransferases (DRMs)-mediated DNA methylation plays key roles in modulating gene expression and maintaining transposable element silencing in soybean. J. Integr. Plant Biol. 67, 1501–1514. https://doi.org/10.1111/jipb.13883.

Zhao, J., Lu, Z., Wang, L., Jin, B., 2021. Plant responses to heat stress: physiology, transcription, noncoding RNAs, and epigenetics. Int. J. Mol. Sci. 22, 1–14. https://doi.org/10.3390/ijms22010117.

Zhong, S., Xu, Y., Yu, C., Zhang, X., Li, L., Ge, H., Ren, G., Wang, Y., Ma, J., Zheng, Y., Zheng, B., 2019. Anaphase-promoting complex/cyclosome regulates RdDM activity by degrading DMS3 in *Arabidopsis*. PNAS 116, 3899–3908. https://doi.org/10.1073/pnas.1816652116.

Zhong, X., Wang, Z.Q., Xiao, R., Wang, Y., Xie, Y., Zhou, X., 2017. iTRAQ analysis of the tobacco leaf proteome reveals that RNA-directed DNA methylation (RdDM) has important roles in defense against geminivirus-betasatellite infection. J. Proteomics 152, 88–101. https://doi.org/10.1016/j.jprot.2016.10.015.

Zhou, R., Kong, L., Yu, X., Ottosen, C.O., Zhao, T., Jiang, F., Wu, Z., 2019. Oxidative damage and antioxidant mechanism in tomatoes responding to drought and heat stress. Acta Physiol. Plant. 41, 1–11. https://doi.org/10.1007/s11738-019-2805-1.

Zushi, K., Kajiwara, S., Matsuzoe, N., 2012. Chlorophyll *a* fluorescence OJIP transient as a tool to characterize and evaluate response to heat and chilling stress in tomato leaf and fruit. Sci. Hortic. 148, 39–46. https://doi.org/10.1016/j.scienta.2012.09.022.